(2)

OFFICE OF NAVAL RESEARCH

Grant No.:N00014-91-J-1303

R&T Code: 1113PO

Technical Report No.: 1

Soluble, Highly Conjugated Derivatives of Polyacetylene from the Ring-Opening Metathesis Polmerization of Monosubstituted Cyclooctatetraenes: Synthesis and the Relationship between Polymer Structure and Physical Properties.

by

Christopher B. Gorman, Eric J. Ginsburg and Robert H. Grubbs

Prepared for Publication in

J. Am. Chem. Soc.

Division of Chemistry and Chemical Engineering
California Institute of Technology
Pasadena, CA 91125

Friday, January 15, 1993

REPORT DOCUMENTATION PAGE

Form Approved OMB No. 0704-0188

1. AGENCY USE ONLY (*leave blank*)	2. REPORT DATE	3. REPORT TYPE AND DATES COVERED
	1/15/93	Technical Report 1/1/92 - 12/31/92

4. TITLE AND SUBTITLE

Soluble, Highly Conjugated Derivatives of Polyacetylene from the Ring-Opening Metathesis Polmerization of Monosubstituted Cyclooctatetraenes: Synthesis and the Relationship between Polymer Structure and Physical Properties.

5. FUNDING NUMBERS

N00014-91-J-1303

6. AUTHOR(S)

Christopher B. Gorman, Eric J. Ginsburg and Robert H. Grubbs

7. PERFORMING ORGANIZATION NAMES (S) AND ADDRESS(ES)

California Institute of Technology
Mail Code: 164-30
Pasadena, CA 91125 USA

8. PERFORMING ORGANIZATION REPORT NUMBER

1

9. SPONSORING/ MONITORING AGENCY NAME(S) AND ADDRESSES(ES)

Office of Naval Research
800 North Quincy Street
Arlington, VA 22217-5000

10. SPONSORING/ MONITORING AGENCY REPORT NUMBER

11. SUPPLEMENTARY NOTES

J. Am. Chem. Soc., in press.

12a. DISTRIBUTION/ AVAILABILITY STATEMENT

unlimited

12b. DISTRIBUTION CODE

13. ABSTRACT (*Maximum 200 words*)

Using well-defined tungsten-based olefin metathesis catalysts, a family of partially substituted polyacetylenes have been synthesized via the ring-opening metathesis polymerization (ROMP) of monosubstituted cyclooctatetraenes (RCOT). These polymers are highly conjugated as evidenced by their visible absorption maxima, they are of high molecular weight as evidenced by gel permeation chromatography, and most members of the family are soluble in the as-synthesized, predominantly cis form. The polymers can be isomerized to the predominantly trans form using heat or light. The rate of thermal isomerization was monitored by visible absorption spectroscopy. Polymers containing, in general, secondary or tertiary groups immediately adjacent to the main chain remain soluble in the trans form and are, in most cases, still highly conjugated.

14. SUBJECT TERMS			15. NUMBER OF PAGES
			16. PRICE CODE
17. SECURITY CLAIFFICATION OF REPORT	18. SECURITY CLASSIFICATION OF THIS PAGE	19. SECURITY CLASSIFICATION OF ABSTRACT	20. LIMITATION OF ABSTRACT
unclassified	unclassified	unclassified	UL

Soluble, Highly Conjugated Derivatives of Polyacetylene from the Ring-Opening Metathesis Polymerization of Monosubstituted Cyclooctatetraenes: Synthesis and the Relationship between Polymer Structure and Physical Properties.

Christopher B. Gorman, Eric J. Ginsburg and Robert H. Grubbs*

Contribution Number 8679 from the

Arnold and Mabel Beckman Laboratories of Chemical Synthesis

California Institute of Technology

Pasadena, CA 91125

Abstract

Using well-defined tungsten-based olefin metathesis catalysts, a family of partially substituted polyacetylenes have been synthesized via the ring-opening metathesis polymerization (ROMP) of monosubstituted cyclooctatetraenes (RCOT). These polymers are highly conjugated as evidenced by their visible absorption maxima, they are of high molecular weight as evidenced by gel permeation chromatography, and most members of the family are soluble in the as-synthesized, predominantly cis form. The polymers can be isomerized to the predominantly trans form using heat or light. The rate of thermal isomerization was monitored by visible absorption spectroscopy. Polymers containing, in general, secondary or tertiary groups immediately adjacent to the main chain remain soluble in the trans form and are, in most cases, still highly conjugated.

Overall, there is a connection between the steric bulk of the side group in polymers of monosubstituted COT's, their effective conjugation length and their

solubility. The side group twists the main chain of the polymer and also induces a preference for cis units in the chain. The tradeoff between conjugation and solubility has been explored, and highly conjugated polyacetylenes that are still soluble have been discovered.

In the solid state, these polymers are observed to be amorphous by wide-angle X-ray scattering and near-infrared scattering. The amorphous nature of these samples correlates with the relatively low temperature cis-trans isomerization in the solid state. Upon iodine-doping, these polymers become electrically conductive, although their conductivities are smaller than those of unsubstituted polyacetylene.

Both empirical and semi-empirical computational methods indicate an increased preference for cis linkages in partially-substituted polyacetylene chains and contain twists around the single-bonds adjacent to the side groups in the polymer chain. The relative magnitude of these twists can be used to rationalize the differences in solubilities of the various polyacetylene derivatives, and these models provide a means of visualizing the conformation of the polymer, at least on its smallest size regime. The computations have also been useful in the rational design of new soluble polyacetylene derivatives with high effective conjugation lengths. By modelling and then synthesizing chains containing *s*-butyl and other secondary groups, these properties have been realized.

Introduction

Conjugated polymers are of current interest because the substantial electronic delocalization along their backbones gives rise to interesting optical[1] and non-linear optical properties[2-4] and allows them to become good electrical conductors, typically when oxidized or reduced.[5, 6] These properties might lead to a variety of applications

including optical signal processing and information storage, lightweight substitutes for metals in batteries[7-9] and materials for solar energy conversion.[10]

Although many different conjugated polymers have been synthesized, a particular obstacle has slowed advancement in the field: most unsubstituted conjugated polymers are unprocessable since they are insoluble and cannot be melted. Overcoming this problem is crucial if conducting polymers are to be widely used. Manipulation of conjugated polymers in solution or in the melt would facilitate the assembly of nonlinear optical waveguides[3, 11] and electronic devices such as solar cells.[10] In contrast to metals, which must be deposited electrochemically or evaporated into place, soluble polymers can be cast from solution. Also, soluble materials make spectroscopic characterization in solution feasible.

The manifestation of electronic delocalization throughout a π-system requires that adjacent monomer units along the backbone be coplanar. This coplanarity tends to make the polymers inflexible and insoluble. This insolubility can be attributed to a combination of a small positive entropy of dissolution (due to lack of conformational mobility in solution) and a small negative enthalpy of dissolution (due to efficient molecular packing or crystallization forces in the solid state). Structural modifications can, however, render a conjugated polymer chain soluble. For example, the attachment of long, flexible, pendant alkyl or alkoxy chains to a rigid chain has induced solubility in polythiophenes,[12-14] polyanilines,[15, 16] poly(phenylene vinylenes)[17] and poly(para-phenylenes).[18, 19] The conformational mobility of the side chains, which act as "bound solvent,"[20] provides enough entropic driving force to carry the rigid polymer chain into solution. Morever, these side chains can also assist solubility by disrupting the packing forces in the solid state.[21]

Soluble derivatives of polyacetylene have been synthesized by polymerization of mono-substituted acetylenes,[22-24] resulting in polymers with a side group attached to

every other carbon on the main chain. In most cases these polymers are soluble, but the optical absorption maximum of the resulting polymer is higher in energy than that observed for polyacetylene, indicating a lower effective conjugation length (e.g. poly-*t*-butyl acetylene is white[22] compared with the blue color of *trans*-polyacetylene). For cases in which iodine-doped conductivities were measured, these soluble polyacetylenes were found to be many orders of magnitude less conductive than polyacetylene.[25-27] This reduction of the effective conjugation of these polymers is postulated to arise from the steric repulsions between adjacent side groups, resulting in twisting of the chain and lowering of the conjugation (Figure 1a). Recent calculations determine the rotation barrier about the single bonds in polyacetylene to be approximately 6 kcal/mol,[28] so loss of planarity in a polyacetylene chain should not be difficult.

We recently reported[29, 30] an approach to a different class of substituted polyacetylenes. It was shown that the ring-opening metathesis polymerization (ROMP) of monosubstituted cyclooctatetraene (RCOT) derivatives (Scheme 1) lead to partially substituted polyacetylenes that were both soluble and highly conjugated. The present paper provides a detailed description of the structure-property relationships uncovered through the synthesis and characterization of a variety of substituted polyacetylenes. Observation of unusual solubility behavior as the steric bulk of the side groups is systematically decreased suggests that this family of polymers encompasses soluble polyacetylene derivatives with a maximized conjugation length. By investigating the solubility-conjugation length tradeoff we have discovered polyacetylenes that are soluble and still highly conjugated.

Results and Discussion

A. Polymer Synthesis and Structural Characterization

We have extended the ROMP[31, 32] of COT[33-35] (1, R=H, Scheme 1) to monosubstituted (RCOT) derivatives to produce polyacetylenes that are substituted, on the average, at one of every eight carbons on the backbone. This strategy leads to less steric crowding of the side groups (Figure 1b) and has resulted in soluble substituted polyacetylenes with the highest effective conjugation lengths measured. Although the exact statistical distribution of side-groups is unknown (because the relative reactivities of the 4 double bonds in the monomer are unknown), the dominant steric interaction in this system, illustrated for the all-trans polymers (Figure 1b) is between the side chain and a β-hydrogen atom. This interaction contrasts with that in polymers of substituted acetylenes in which side groups can interact in a stronger repulsive manner.

The tungsten alkylidenes 2[36] and 3[37] both polymerized a variety of monosubstituted cyclooctatetraenes. Either catalyst (dissolved in a minimum of solvent) was mixed with the monomer (a yellow liquid) as described in the experimental section, initially producing a dark viscous solution and finally a film that was generally strong and flexible. Polymers were initially synthesized in the predominantly cis configuration and could then be isomerized to the predominantly trans configuration.

The molecular weights of those polymers that were soluble in the initially synthesized, cis configuration were estimated by gel permeation chromatography (GPC) calibrated versus polystyrene standards (Table 1). Although high molecular weights were consistently obtained, the polymerization reaction afforded little control over molecular weight. Partial cis to trans isomerization resulted in some loss of solubility for certain polymers and, for polymers that were soluble in both the cis and trans forms, an apparent increase in molecular weight versus polystyrene. Presumably, the polymer chains

became more rigid upon isomerization, and the subsequent increase in hydrodynamic radius is reflected as an increase in apparent molecular weight. For consistency, the molecular weights reported here are for polymer samples dissolved in the chromatography solvent within one hour after synthesis. Light scattering measurements on *cis*-poly-*t*-butylCOT indicated that the polymer had a weight average molecular weight of approximately 20,000 (approximately 125 monomer units or 500 double bonds, about one-half the value estimated by GPC). This polymer is relatively non-conjugated and was the only polymer synthesized that did not strongly absorb the light used in the light scattering experiment (632.8 nm).

Another factor affecting the molecular weight and the polymer yield is the extent to which the growing chain undergoes cycloextrusion of a substituted benzene (Scheme 2). This side reaction, also termed "back-biting", is strongly driven by the formation of an aromatic ring, and does not terminate the polymerization, but does reduce the molecular weight of the polymer. In dilute solution, in which the local concentration of polymer olefin units is high relative to monomer concentration, cycloextrusion can become a significant process.[35] Thus, polymerizations are generally performed in neat monomer. Cycloextrusion also reduces the number of side groups in the polymer and increases the uncertainty in the side group placement along the chain by adding olefin units between side groups. Cycloextrusion events are expected to principally remove the side group and produce a substituted benzene since the production of unsubstituted benzene would require metathesis of a trisubstituted double bond - unlikely given the steric requirements of these catalysts.[31] In addition, when any aromatics that were produced were rinsed from a film after polymerization (along with catalyst residues), the stoichiometry of the polymer no longer corresponded to that of the monomer, complicating the elemental analysis. Nevertheless, both the extent of monomer conversion and the percentage of cycloextrusion can be estimated by NMR (see experimental section). In almost all trials, greater than 85% of the monomer was ring-

opened and cycloextrusion occurred to 7-16%. Variations in these values did not significantly affect any of the measured physical properties of the polymers (with the exception of NMR spectra and molecular weights).

Solubility behavior. Many of these polymers were soluble in common organics such as tetrahydrofuran, methylene chloride, chloroform, benzene, toluene. No dramatic differences in solubility were observed among these solvents. No polymers were soluble in saturated hydrocarbons (pentane and hexane) or alcohols (methanol). Several empirical relationships could be drawn between the structure of the side group and the solubility of the resulting polymer. Polymers containing *n*-alkyl side chains, even that with a length of 18 carbons (poly-*n*-octadecylCOT) were found to be soluble in the cis form, but almost completely insoluble in the trans form. Poly-neopentylCOT ($R = -CH_2C(CH_3)_3$, $R_\alpha = -CH_2-$) and poly-2-ethylhexylCOT ($R = -CH_2CH(C_2H_5)(C_4H_9)$, $R_\alpha = -CH_2-$) display solubility behavior much like the poly-*n*-alkylCOT polymers ($R = -CH_2(CH_2)_nH$, $R_\alpha = -CH_2-$ also). The same basic behavior is observed for alkoxy (methoxy, *t* -butoxy, $R_\alpha = -O-$) and phenyl substituted derivatives. Solubility of these cis polymers was often short lived due to facile isomerization to the insoluble trans isomer, even in the solid state. Polymers containing a secondary (e.g. *s* -butyl, *i*-propyl, cyclopentyl, $R_\alpha = -CHR'R''$) or tertiary (trimethylsilyl, *t*-butyl, $R_\alpha = -ER'R''R'''$, E = C, Si) substituent adjacent to the backbone were soluble in both the predominantly cis and predominantly trans forms. Thus, it appears that the steric bulk of the side chain at the position adjacent to the double bond (α) determines the solubility of the polymer.

Since isomerization from cis to trans is facile for polymers containing $R_\alpha = -CH_2-$ or $R_\alpha = -O-$, these *cis*-polymer solutions had to be handled with minimal exposure to light and stored at low temperature (- 50° C). Isomerization in solution resulted in a blue suspension which could not be filtered through a 0.5 μm filter, but could be recast into a

free-standing film. Even in the solid state, under inert atmosphere, films would isomerize at room temperature and ambient light, rendering the polymer insoluble. For example, a week after synthesis, differential scanning calorimetry of a film of poly-*n*-octylCOT kept under inert atmosphere under ambient light and temperature revealed no exotherm assigned to cis/trans isomerization. Nevertheless, these polymers can serve as soluble "precursors" to the trans polymer and are of interest in their own right as soluble conjugated polymers.

Proton NMR. Proton NMR data were collected for all of the polymers in the cis form . Resonances due to residual monomer and cycloextrusion product weere identified and integrated to determine the percentage of conversion of monomer and the percentage of cycloextrusion product (experimental section). Resonances attributed to the polymer side chains were observed and were shifted slightly downfield from those of the monomer. A broad series of resonances between 5.6 and 7.0 ppm (C_6D_6) was observed, corresponding to protons on the main chain. All of these resonances shifted downfield as the polymer isomerized from cis to trans. This shift is consistent with the increased electron delocalization expected upon isomerization. Two resonances were observed for each of the side chain protons in the trans form of all of those polymers that were soluble in this form. These are thought to correspond to cis-trans and trans-trans diads in the polymer and are discussed more thoroughly below. Figure 2 compares proton NMR spectra of isopropylCOT, *cis*-polyisopropylCOT and *trans*-polyisopropylCOT. Comparison of the cis and trans NMR spectra for other soluble polymers is possible but more difficult for more complicated side chains due to overlapping resonances. Typically, the methine proton resonance (e.g. -CHRR') in the side chain is the best resolved peak.

Resonance Raman Spectroscopy. Raman spectroscopy provides evidence that these polymers possess a polyacetylene backbone. Two strongly resonance-enhanced

symmetric stretches (Fig 3) observed (Table 3) are assigned as A_g(C-C) (ν_1) and A_g(C=C) (ν_2) as are observed in *trans*--polyacetylene.[38] Corresponding infrared stretches, observed at 740 cm^{-1} for *cis*-polyacetylene and 1015 cm^{-1} for *trans*-polyacetylene[39] are generally obscured by bands due to the side group. The exact position of these Raman bands are sensitive to the degree of conjugation of the polymer and the excitation wavelength employed.[38] Raman spectra characteristic of *cis*-polyacetylene were not observed, possibly because light and/or heating due to the laser isomerized the samples.

B. Cis/Trans Isomerization

Based upon calorimetry measurements, the trans configuration of unsubstituted polyacetylene is more stable than the cis configuration by approximately 0.85 kcal/mol of CH units .[40] Isomerization can be induced either by heating[41-43] or by doping.[44, 45] Photochemical isomerization has not been reported for polyacetylene in the solid state, but it can be accomplished in solution with some of these substituted polymers. The thermal isomerization of polyacetylene has been studied in the solid state and is complicated, following no discrete reaction order. The isomerization in crystalline regions and amorphous regions is postulated to proceed with different activation energies.[39] At early stages of isomerization (presumably in the amorphous regions where chains can move more freely), Tanaka et al. have found that the process is activated by about 17 kcal/mol, although barriers as low as 11 kcal/mol have been reported.[46] At higher conversion (presumably in the crystalline regions of the polymer), this activation barrier increases considerably. The relationship between the morphology of the polymer film and the isomerization barrier in the solid state will be discussed below when interpreting solid-state isomerization data for poly-RCOT's.

Kinetics of Cis/Trans Isomerization. The thermal and photochemical isomerization of soluble poly-RCOT's in solution has been monitored by visible absorption spectroscopy. The lower isomerization temperatures reported here are

contrasted with the more extreme thermal conditions used to isomerize crystalline polyacetylene in the solid state (e.g. heating at 150 °C). It is believed that chemical defects can be created during this thermal isomerization process.[42] We observed no evidence of this phenomenon (by NMR) when soluble polyacetylenes were isomerized in solution.

In the completely (cis and trans) soluble polymers (i.e. those containing a secondary or tertiary side group), the visible absorptions due to each isomer are well separated in energy, allowing the photochemical cis/trans isomerization of poly-trimethylsilylCOT to be followed in solution.[30] Here, the absorption corresponds to a collection of olefin units with an effective conjugation length of 15-20 double bonds (discussed in more detail below). An isosbestic point was observed, suggesting that either all of the olefins comprising this chromophore were isomerizing simultaneously in solution without detectable intermediates or that no observable change in chromophore absorption occured until some threshold number of individual double bonds had isomerized. Tanaka et al. have observed an isosbestic point in the visible absorption spectrum upon thermal cis/trans isomerization of polyacetylene in the solid state.[46] Simultaneous isomerization of multiple double bonds in polyenes[47, 48] and other conjugated molecules[49] has been reported in the literature. Trajectories in which more than one double bond is isomerized at a time are proposed since multiple isomerization trajectories often allow for less motion than separate single bond isomerizations.

The thermal isomerization of poly-*s*-butylCOT in solution was monitored by visible absorption spectroscopy (Figure 4). An isosbestic point was observed throughout most of the reaction. Near the end of the reaction, large increases in extinction coefficient were observed with a concomitant loss of the isosbestic point, possibly due to some large scale conformational change.

Rates of isomerization were determined by monitoring the change in absorbance of the cis and trans chromophores of poly-*s*-butylCOT. The rate of increase in absorption at 560 nm of the *trans*-chromophore was measured. First order kinetics were observed, with the molarity considered to be moles of "chromophores" (i.e. effectively 15-20 conjugated double bonds, see below). An Arrhenius plot of rate at four different temperatures from 45 °C-75 °C gave an energy of activation $E_a = 21.3 \pm 0.4$ kcal/mol with $A = 2.4 \times 10^{10}$. An Eyring plot gave activation parameters of $\Delta H^{\ddagger} = 20.6 \pm 2.1$ kcal/mol and $\Delta S^{\ddagger} = -13.3 \pm 4.5$ cal/mol•K. (Fig 5) Isomerization rates were observed to be similar in benzene and THF, suggesting a nonpolar transition state. These activation energies are in the range reported for polyacetylene in the solid state. This relatively low barrier of activation is not surprising since a twisted biradical transition state, often proposed for olefin isomerization, would be stabilized by delocalization of the biradicals within the π-system.

The lowering of cis/trans isomerization barriers due to biradical delocalization has been observed for stilbenes ($\Delta G^{\ddagger} = 55.1$ kcal/mol at 723K),[50] cumulenes ($\Delta G^{\ddagger} = 30$ {373 K}, 27.5 {298 K}, and 20 {393 K} kcal/mol for 4, 5, and 6 carbon cumulenes, respectively),[50] and recently in rationally designed polyene model compounds ($\Delta H^{\ddagger}$(kcal/mol), $\Delta S^{\ddagger}$ (cal/mol•K) of 38.9, -6.0; 32.1, -4.4; 27.5, -4.4 for a semi-rigid triene, pentaene, and heptaene, respectively).[51] In comparison ethylene (CHD=CHD) has a 65 kcal/mol barrier for isomerization at 723K.[50] Since the twisted biradical transition state can be thought of as a pair of mobile, delocalized solitons rather than as two localized spins, the transition state in polyacetylene is an extreme example of stabilization due to delocalization.

Dynamic Cis/trans Isomerization of the Trisubstituted Double Bond. Despite the energetic preference for a double bond to be trans, residual cis double bonds were observed in "fully" isomerized polyacetylene. These units comprise an estimated 5-7%

of so-called *trans*-polyacetylene,[39] and their effect upon carrier (soliton) formation has been discussed.[41] Residual cis units in *trans*-polyacetylene (and trans units in *cis*-) will undoubtedly influence the physical properties of the polymer.

The existence of residual cis units in the "*trans*"-poly-RCOT's was indicated when ^{1}H NMR spectra of soluble polymers in the cis and trans form were compared. As mentioned above, resonances due to main-chain protons were broad and generally uninformative. However, two resonances for each of the side chain protons in the trans polymer were resolved, yet only one resonance in the cis polymer was observed. These resonances are well separated and particularly easy to observe for the methine (e.g. -CH-) proton of the side group in the spectrum of *trans*-poly-*s*-butylCOT (Figure 6). The most upfield resonance was observed to dissappear upon isomerization and is assigned to a cis/cis diad in the polymer. The two resonances appearing upon isomerization are assigned to cis/trans and trans/trans diads in the polymer. No NOE enhancement of either resonance was observed upon irradiation of the downfield, main-chain protons. Assuming they are at equillibrium (see below), integration of the two methine signals in the trans polymer at 50 °C determined the difference in energy of the diads to be small (0.8 kcal/mol) with a larger integration for the upfield signal. Computationally derived (AM1) heats-of-formation of model compounds indicate that trisubstituted double bonds in model polyenes prefer to be cis with respect to the main chain (see below). Leclerc et al. have observed that side groups in polymers of substituted acetylenes also appear to increase the cis content (again with respect to the main chain) of the polymer.[15] Based upon this evidence, the larger upfield resonance is assigned to the cis/trans diad. Interconversion of the cis/trans and trans/trans diads was revealed by a magnetization transfer experiment on *trans*-poly-*s*-butylCOT. $\Delta G^{\ddagger} = 18.9 \pm 0.4$ kcal/mol was measured at 50 °C in d_6-benzene for conversion from the cis/trans to the trans/trans diad. This activation energy corresponds to an interconversion rate of $\approx 1\ s^{-1}$ at this temperature.

Cis/Trans Preference for the Trisubstituted Double Bond. Despite the fact that the double bonds in unsubstituted polyacetylene have a preference to be trans, it does not necessarily follow that the trisubstituted double bond in substituted polymers need have such a strong preference. The relative energies of cis/cis, cis/trans and trans/trans diads were determined by comparing the heats of formation of the geometry optimized model tetraenes, **4** (Figure 7) using the semi-empirical Hamiltonian AM1 in AMPAC.[52] These values are displayed graphically in Figure 8 for each of the three isomers and the difference in heat of formation between isomers is tabulated in Table 2. This computation predicts that not every double bond has such a strong preference to be trans with respect to the main chain. The first isomerization (cc → ct, the disubstituted double bond) is always exothermic. However, only in a few cases (R = MeO, Np) is the isomerization of the trisubstituted double bond exothermic.

C. Structure/Property Relationships for the Polymers in Solution

Visible Absorption Spectra. All of the polymers display intense absorptions ($\varepsilon \approx 10^3$ $cm^{-1}M^{-1}$) in the visible spectrum. The absorption maxima for both the predominantly cis and trans forms of the polymer are tabulated in Table 3. It was noted above that some of these polymers are not soluble in the trans form. Nevertheless, upon isomerization of very dilute (< 10^{-5} M) solutions of these polymers, visually homogeneous blue solutions resulted and their optical absorption maxima are reported. (Fig. 9) Presumably they contain aggregated material since filtration of these solutions (5 μm filter) typically resulted in a purple solution (λ_{max} = 580±10 nm) that was of low molecular weight (M_n < 5000, GPC vs. polystyrene standards).

Optical absorption spectra of conjugated polyenes are known to differ between the solid-state and solution. A red shift in the lowest energy visible absorption maximum has

been observed in β-carotene (a biopolyene) upon aggregation in the bilayers of lipid vesicles.[53] Polyene spectra in the solid state are red-shifted compared to those in solution.[54] Also, the lowest energy absorption peak in polyacetylene undergoes a red-shift when pressure is applied to the sample.[55] This red-shift with pressure can be attributed in part to increased planarity of the chains with increasing density, but it is also possible that the solid polyenes are a more polarizable medium than typical organic solvents. Neither ground nor excited states of polyenes have a dipole moment, and it has been noted that polyene spectra are not very sensitive to solvent polarity but rather solvent polarizability.[56] Optical absorptions of poly-RCOT's shift 30-50 nm to the red when comparing their solution spectra and spectra of thin films. For example, *trans*-poly-*n*-octylCOT has a broad absorption centered around 650 nm in the solid state and 620 nm in THF solution. A red-shift was also observed in more polarizable solvents. Although no significant solvatochromic effect was observed in the optical absorption spectra of poly-RCOT's as solvent polarity changed (e.g. from THF to CH_2Cl_2 to benzene), a 30 nm red-shift was observed in the absorbance maximum of *trans*-poly-*s*-butylCOT dissolved in CS_2 (λ_{max} = 586 nm) versus THF (λ_{max} = 556 nm). This solvent is not polar but is very polarizable (i.e. the solvent electron cloud can respond to the high frequency transient dipole induced by an electronic transition) and stabilizes the transition in the polymer, presumably because it is also very polarizable. The possible effect of polymer polarizability upon attractions between polymer chains and thus upon polymer solubility will be discussed.

The optical absorption maxima of these polymers can be used as an indication of the effective conjugation length (n) of the double bonds in the main chain. This quantity has been defined by extrapolation of optical absorption maxima in solution for discrete all-trans polyenes of the form R-$(CH{=}CH)_n$-R. The lowest energy optical absorption of these molecules shifts to lower energy upon increasing the length of the molecule.[57-64] It has been shown[54, 65-67] that this optical absorption maximum (λ_{max}) can be related to the

conjugation length by the function $\lambda_{max} = a + b/n$. The value of a and b depends upon a number of factors, including solvent and the end groups on the polyene. Interestingly, extrapolating the optical absorption maxima for polyenes to the infinite-chain value gives a lower energy than the optical absorption maximum observed for polyacetylene. Several workers[54, 68] have taken this observation to suggest that conformational or other defects limit the conjugation in polyacetylene to an effective conjugation length of approximately 30 double bonds.

Based upon an extrapolation of optical absorption data for all trans polyenes in the range of 2-10 double bonds,[54, 65-67] those polyRCOT's with methylene units adjacent to the main chain have an effective conjugation length of 25-30 double bonds. Spectra of thin films are similar to that for polyacetylene, indicating a similar the effective conjugation length. The trans polymers with more bulky substituents, especially adjacent to the main chain, have slightly blue-shifted λ_{max} (R = isopropyl, *s*-butyl, cyclopentyl, TMS), implying a slightly reduced effective conjugation length of 20-25 double bonds. The bulky side group in *trans*-poly-*t*-butylCOT severely limits conjugation to perhaps 10 double bonds. Its spectrum is directly comparable to the most intense transition recorded in dichloromethane of an all *trans*-polyene with 10 double bonds.[69] Given that alkyl side groups change the optical absorption of polyenes by less than 10 nm,[70] suggesting that their electronic effect on the transition is minimal, a polymer such as *trans*-poly-*s*-butylCOT displays the highest observed effective conjugation length for a ***soluble*** polyacetylene.

Efforts have been undertaken to observe the spectral signature of so-called "mid-gap states" in these polymers after doping. Initial experiments using a diode array spectrophotometer in the visible confirmed that the doped species, recognizable as an instantaneous change in color from purple to blue as the dopant ($NOPF_6$) was added to *trans*-poly-*s*-butylCOT in $CHCl_3$,[71] decomposed to an unidentified brown species over

the course of 5-10 minutes at room temperature. At -78 °C, the doped species does not form, at least over the course of 5-10 minutes as suggested by the lack of change in the color of the solution. However, at -20 °C, the species forms, and sealed tubes of the doped *trans*-poly-*s*-butylCOT can be kept at -50 °C for weeks. This species is intensely colored in the visible and near infrared. Dilution to a reasonable concentration for spectroscopy ($\approx 10^{-4}$ to 10^{-5} M) unfortunately resulted in decomposition, probably because the sample was sensitive to trace impurities. More conclusive results have been obtained on thin films of poly-RCOT's.[72]

The Solubility/Conjugation Length Tradeoff. The optical absorption and solubility data of the *trans*-poly-RCOT's indicate that a compromise must be made between conjugation length and solubility in polyacetylene derivatives. More conjugated polymers tend to be less soluble. Specifically, poly-RCOT's in which there is a methylene (R_α = -CH_2-) unit immediately adjacent to the main chain including *n*-alkyl substituted polymers, polyneopentylCOT (R = -$CH_2(CH_3)_3$) and poly-2-ethylhexylCOT (R = -$CH_2CH(C_2H_5)(C_4H_9)$) have an effective conjugation length similar to polyacetylene. These polymers (excluding R = CH_3) are solubilized in the cis form, but not in the trans form. After isomerization, the majority of the trans material will not pass through a 5 μm filter. Polyenes containing cis double bonds have been observed to be more soluble than all trans polyenes,[69] although the latter insolubility was attributed to covalent cross-linking. If such cross-links are present in the *trans*-polyRCOT's, they do not result in a decrease in λ_{max} compared to polyacetylene, and the conclusion that unsubstituted, conjugated all-trans polyenes are insoluble because they are crosslinked implies that *trans*-polyacetylene is crosslinked in the solid state. It is conceivable that these polymers might undergo radical crosslinking at the allylic site on the side group. However, a random copolymer synthesized from 50% trimethylsilylCOT/50% *n*-octylCOT was found to be soluble as long as it remained under inert atmosphere (see

below), speaking against this possibility. An alternative explanation is that attractive noncovalent interactions are sufficient to aggregate long polyenes.

A secondary or tertiary group adjacent to the main chain does reduce the conjugation, but it affords solubility in both the cis and trans forms of the polymer. Empirically, only steric effects immediately adjacent to the main chain affect conjugation and solubility. Several polymers were synthesized to test these statements. *Trans*-polyneopentylCOT, in which a *t*-butyl group is spaced one unit away from the main chain, behaves like *trans*-poly-*n*-alkylCOT. *Trans*-poly-*t*-butylCOT is soluble, but not highly conjugated. Pulling this bulky group back a small amount as in *trans*-polytrimethylsilylCOT increases the conjugation considerably. This increase is attributed to the longer Si-C bond compared to a C-C bond.[73] Use of a secondary group (as in *trans*-poly-*s*-butylCOT) has so far provided the highest possible conjugation length without loss of solubility. The smaller, but still secondary side group in *trans*-poly-cyclopropylCOT afforded an insoluble polymer similar to the *trans*-poly-*n*-alkylCOT's. Overall, the steric effect of the side group determines the conjugation of the polymer.

The simplest explanation for these data is that the side group causes the polymer chain to twist, affording solubility, but with a loss of conjugation. A flexible side group and this twist will serve to increase the entropy of dissolution of the polymer, a common approach for solubilizing rigid polymers.[20] It should be noted that the poly-RCOT's behave differently than the polythiophenes.[13, 14] Attachment of short *n*-alkyl side groups (e.g. *n*-hexyl, *n*-octyl) serves to solubilize a polythiophene chain, but even the attachment of *n*-octadecyl (C_{18}) chains to *trans*-polyacetylene does not solubilize it. It is possible that strong Van der Waals interactions between polyacetylene chains may play a role. It has been illustrated in the literature[74, 75] and by some of the optical absorption data above that polyene chains are very polarizable and their polarizability increases with conjugation length. It is expected that the unit polarizability of polyacetylene could be

higher than that of the more aromatic polythiophene. Thus, a reduction in conjugation length due to chain twisting may result in a reduction in polarizability leading to a reduction in Van der Waals forces.[76] The relative contributions to the energy of dissolution due to enthalpy and entropy are unclear.

Copolymers. It has already been demonstrated that COT can be copolymerized with 1,5-cyclooctadiene to give a random copolymer containing segments of reduced conjugation length and with norbornene to give a block copolymer containing highly conjugated segments,[77] but neither is both soluble and highly conjugated. By copolymerizing two monosubstituted COT derivatives, one which homopolymerizes to give a soluble polymer and one which homopolymerizes to give an insoluble polymer (both in the trans form), it should be possible to "tailor" the effective conjugation length of the resulting polymer by adjusting the ratio of the two monomers. Although no information on relative reactivities of monomers is available, the copolymerization of *n*-octylCOT or *n*-butylCOT (monomers in the latter category) with trimethylsilylCOT (a monomer in the former category) we have synthesized a family of polymers in which the effective conjugation length of the resulting copolymer increases monotonically with the amount of the *n*-octylCOT or *n*-butylCOT in the monomer feed (Figure 10). For both families of copolymers, as the absorption maximum of the copolymer reaches approximately 580 nm, the polymer becomes insoluble. Although copolymers derived from 40% or 50% trimethylsilylCOT in the monomer feed were completely soluble in concentrated (≈ 1 mg/mL) solutions in both the cis and trans forms, copolymers synthesized with a smaller ratio of this monomer may be aggregated in the trans form, much like *trans*-poly-*n*-butylCOT or *trans*-poly-*n*-octylCOT. As was mentioned above, the solubility of a copolymer containing an *n*-alkyl group implies that poly-*n*-alkylCOT's do not crosslink via the allylic sites on the side groups.

It has been reported that solutions of polyacetylene derivatives with optical absorption maxima of around 580 nm are not homogeneous. This phenomenon has been observed in polyacetylene block and graft copolymers in which one block is a solubilizing tail.[78] In most cases, this modification permitted preparation of solutions that have facilitated a variety of studies of the linear[79, 80] and nonlinear[81, 82] optical properties as well as photoinduced absorption studies[83] of polyacetylene segments in solution. There is evidence however, that the polyacetylene segments in these polymer solutions are aggregated or crosslinked.[84, 85] Overall, these data, combined with poly-RCOT data support the contention that there is a maximum soluble conjugation length possible for polyacetylene derivatives.

D. Solid State Properties

Probes of film morphology. Polyacetylene films, synthesized from either acetylene or COT[35] are highly crystalline. In contrast, films of poly-R-COT (except for R = methyl, which still appears somewhat crystalline) show only an amorphous halo by wide-angle X-ray scattering. This observation is in contrast to polyCOT, in which lattice spacings could be determined from several sharp lines observed. Scanning electron microscopy (SEM) of the surfaces and freeze-fracture cross sections of the films showed them to be completely smooth, with no detectable fibrillar morphologies or other features of size 1 μm or larger. In contrast, films of polyCOT have smooth surfaces but fibrillar interiors.[35]

Absorption spectra of polyCOT films show high optical density (>1 for 20 μm thick films) even at lower energy than the true absorption edge[86] in the near IR. The apparent absorption decreases with increasing wavelength but extends out beyond 2000 nm. This apparent absorption is actually due to scattering as shown by laser light

scattering observations. The loss coefficient of such films is estimated to be > 500 cm^{-1} at 1500 nm. This scattering arises from internal optical inhomogeneities in the polymer associated with the semi-crystalline, fibrillar morphology. In contrast, films of poly-*n*-butylCOT show very clean transmission in the near IR. Films 100 μm thick show a sharp absorption edge at ~900 nm and little absorption beyond 1000 nm. For poly-*n*-butylCOT films, the loss coefficient is estimated to be < 0.2 cm^{-1} at 1500 nm. The greatly reduced scattering loss indicates that partial substitution of polyacetylene with butyl groups has resulted in a more homogeneous morphology. This low scattering will be important if polyacetylene is to be used in optical applications and has been discussed in terms of nonlinear optical applications for these polymers.[87]

Differential Scanning Calorimetry. Films of *cis*-poly-R-COT display an irreversible exotherm between 100-165 °C that does not correspond to any weight loss as shown by thermal gravimetric analysis (Table 3). This exotherm is attributed to cis/trans isomerization as observed at 150 °C in polyacetylene[40] and poly-COT (i.e. R = H). Since most side groups on the polymer render it amorphous, it appears that crystalline polyacetylene is more difficult to isomerize than amorphous polyacetylene. This conclusion is supported by the DSC of the amorphous polyacetylene produced by the precursor route of Feast and Edwards.[88] This form of polyacetylene is reported to have an isomerization temperature of 117 °C.[89] The soluble poly-R-COT's with a reduced conjugation length have higher isomerization temperatures than the less-twisted derivatives. This behavior is understandable since a polyene sequence with a longer conjugation length should be easier to isomerize than a polyene sequence with a shorter conjugation length.[51] Thus, both intrachain and interchain effects are taken into account when rationalizing the solid-state isomerization behavior of these polymer films.

Conductivity of Free-standing Films. Few trends in the iodine-doped conductivities of films of different poly-R-COT's could be determined (Table 3). None

of the substituted polymers has an improved conductivity over the parent (i.e. R = H). This is expected, since side groups should reduce both intrachain and interchain carrier transport by reducing conjugation due to twisting and interchain hopping via loss of crystallinity. In general, more conjugated polymers tend to be more conductive. Anomalies exist, however. For example, even though it would be logical that side group interference with electron hopping would be higher in poly-*n*-octylCOT than in poly-*n*-butylCOT, the former has a reproducibly higher conductivity by two orders of magnitude. There is no evidence that the conjugation in poly-*n*-butylCOT is reduced compared to poly-*n*-octylCOT. It was not possible to dope poly-*t*-butylCOT with iodine.[72] In contrast, poly-*t*-butoxyCOT absorbed a substantial amount of iodine, yet it too displayed a low conductivity after doping.

Polyacetylene is known to isomerize upon doping,[44, 45] and iodine-isomerized *cis*-polyacetylene is reported to have a higher conductivity than similarly treated *trans*-polyacetylene.[90] However, a substantial increase in conductivity was observed in poly-neopentylCOT and poly-*s*-butylCOT if the polymer was isomerized in solution (even if it then precipitated) and was then recast before doping. Isomerization in solution is perhaps a more gentle process than thermal isomerization in the solid state, resulting in less destruction to the polymer film.

E. Computational Studies on Model Oligomers

Chain Twisting - Static Picture. A model for local polymer conformation was developed using both force-field (MM2)[91] and semiempirical quantum mechanics (AM1)[52] calculations on model oligomers of the type **5** and **6** (Figure 11). For various side groups, the geometry of these oligomers was optimized and the effect of the side group upon the conformation of the main chain was examined. Side group placement on

the polyene is 7 and 9 carbons apart. Polymerization of a monosubstituted COT will give side groups spaced, on the average, every eight carbons apart. Assuming the trisubstituted olefin in the monosubstituted COT does not react in a polymerization, these side groups could get as close as 4 carbons apart. We have not modelled this case. However, since these two side groups are not directly attached to each other, a force-field calculation will recognize their interaction only through the Van der Waals energy term, and, especially for small (second row) atoms, this term rapidly becomes negligible within a few Angstroms.[92]

Although some force field parameterizations tabulate interactions based upon atom hybridizations, treating all C_{sp2}-C_{sp2} interactions identically in a polyene is not acceptable. The bond lengths of polyenes alternate (i.e. C-C is ≈ 1.46 Å and C=C is ≈ 1.34 Å). In the version of MM2 employed here, interactions are tabulated for atoms bonded in specific ways. Thus, for example, the torsion potential of a single bond between two double bonds (e.g. $C_{sp2} = C_{sp2} - C_{sp2} = C_{sp2}$).is specifically tabulated. Brédas and Heeger have used ab initio routines to calculate the gas-phase torsion potential of polyacetylene oligomers to be about 6 kcal/mol. This value is comparable to the barriers calculated for single-bond rotation in butadiene, in previous calculations on *cis*- and *trans*-polyacetylene,[93] and in the oligomers discussed here.

Similar geometry-optimized structures were found using both MM2 and AM1. In these structures, the two single bonds in the main chain adjacent to each of the three substituents are twisted out of planarity. Two dihedral angles adjacent to the center substituent (Fig 12) are reported in Table 4. No bond lengths or angles are dramatically different from those previously reported for polyenes. Furthermore, dihedral angles around single bonds further removed from the substituent as well as dihedral angles about all double bonds deviate less than 5° from planarity. It is noteworthy that MM2 and AM1 results are similar. MM2 treats each single bond as independent of conjugation length whereas

AM1 performs a full Hartree-Fock calculation on the molecule producing bond-orders which could be dependent on chain size. Nevertheless, similar twist angles are found for an arbitrary conjugation length, and this computation qualitatively agrees with previous geometry optimizations on polyenes and polyacetylenes.[28] Thus, conjugation length does not affect single bond rotation potentials, although it does affect double bond isomerization potentials since these motions do not occur solely via the ground electronic state of the molecule.

Empirically, it is observed that twists in both Θ_1 and Θ_2 are large in the geometry-optimized models of the soluble polymers. In contrast, in the model of poly-*t*-butoxyCOT, Θ_1 is large, but Θ_2 is not, and, experimentally, the polymer is not soluble. Based upon the good correlation between polymer solubility and chain twist, we have placed a line across a bar graph of twist angles indicating the minimum magnitude of twist in a model compound that corresponds to a soluble polymer (Figure 13). If both Θ_1 and Θ_2 are sufficiently large, the polymer is predicted to be soluble. Interestingly, the twists in the model of *trans*-polycyclopropylCOT were very close to the limit drawn on the graph, but this polymer was not soluble. Thus, we have found this model useful in evaluating the limits of solubility for highly conjugated polyacetylene derivatives.

Calculations were performed on molecules of type **6** (Figure 11) because of the evidence presented above that the trisubstituted double bonds in the isomerized polymer can often be cis with respect to the main chain. These models are twisted as well, and twists around single bonds adjacent to cis double bonds are larger than those adjacent to trans double bonds. Overall, the conformation of the real polymer includes nonplanar segments containing both cis and trans double bonds.

Dynamic Picture of Chain Twisting. Energy minimized structures do not address the extent to which the solubility-inducing kink is a static or a dynamic phenomenon. The question remains: are the substituted polycyclooctatetraenes rigid but

kinked molecules, or does the attachment of substituents make the backbone flexible by providing hinge points about which the polymer rotates? In the absence of experimental data, molecular dynamics calculations, which are used to explore the evolution of molecular motion over time,[94, 95] can provide some insight. Using the MM2 force field, molecular dynamics simulations of the model compound **5** have been conducted. Models of four different poly-RCOT trimers were held at 300 K for a simulated 20 picoseconds and the geometry was allowed to vary. The torsion angle, Θ_1, was sampled every 10 femtoseconds (Figure 14). In general, the dihedral angles remain close to transoid planarity (180°) rocking from side to side during the run. The single bond in the *n*-butyl oligomer spends more time in a nonplanar conformation than the unsubstituted (i.e. R = H) oligomer. The single bond in the *s*-butyl oligomer samples even more nonplanar conformations. The single bond in the *t*-butyl oligomer is found in both transoid ($|180°| \leq \theta_1 \leq |90°|$) and cisoid ($|90°| \leq \theta_1 \leq |0°|$) conformations. During the run tabulated in Figure 14, the *t*-butyl substituent was never coplanar with the main chain. Thus, it was found only on one side of the chain, and Θ_1 assumed only negative values. In longer runs or at higher temperatures, the *t*-butyl substituent should eventually move to the other side. In the series *n*-butyl to *s*-butyl to *t*-butyl, the dynamics indicate that the model spends more and more time in increasingly varied conformations. Thus, flexibility increases with the steric bulk of the substituent. This result, coupled with the solubility behavior noted above, suggests the importance of entropy in the dissolution of these polymers.

Experimental

Monomer Syntheses. All syntheses of substituted cyclooctatetraenes are air- and moisture-sensitive and were performed using standard Schlenk techniques under argon purified by passage through columns of BASF RS-11 (Chemalog) and Linde 4Å

molecular sieves. NMR spectra were recorded with either a JEOL FX-90Q (89.60 MHz ^{1}H; 22.51 MHz ^{13}C), a Bruker AM-500 (500.14 MHz ^{1}H, 125.13 MHz ^{13}C) or a JEOL GX-400 (399.65 MHz ^{1}H, 100.40 MHz ^{13}C) spectrometer. Chemical shifts were referenced to the chemical shift of the residual protons of the solvent with respect to tetramethylsilane. Gas chromatography analyses (VPC) were performed on a Shimadzu GC-Mini-2 flame-ionization instrument with a 50 m capillary column equipped with a Hewlett-Packard model 339A integrator. Low resolution mass spectra were obtained on a Hewlett-Packard Series 5970 mass selective detector in conjunction with a Series 5890 GC equipped with a 15 m SE-30 capillary column. Preparative VPC was performed on a Varian 920 Aerograph with a thermal conductivity detector equipped with a Hewlett Packard 7127A strip recorder. Thin-layer chromatography (TLC) was performed on precoated TLC plates (silica gel 60 F-254, EM Reagents). Flash chromatography was by the method of Still et al.,[96] using silica gel 60 (230-400 mesh ATM, EM Reagents). Elemental analysis was performed at the analytical facilities of the California Institute of Technology.

Pentane, tetrahydrofuran, toluene and diethyl ether were distilled from sodium benzophenone ketyl. Methylene chloride and chloroform were vacuum transferred from calcium hydride. COT was purchased from Strem or was received as a gift from BASF and was distilled from calcium hydride before use. All other reagents were purchased from Aldrich unless otherwise noted.

Bromocyclooctatetraene and methyl cyclooctatetraene were synthesized by the method of Gasteiger, et al.[97] $[n\text{-}Bu_3P{\bullet}CuI]_4$[98] was synthesized as described in the literature. MethoxyCOT and *t*-butoxyCOT were synthesized as described in the literature[99] except that THF was used as the solvent for the reaction instead of DMSO. *p*-MethoxyphenylCOT and cyclopropylCOT were synthesized as described in the literature[100] as were trimethylsilylCOT[101] and *t*-butylCOT.[102] *n*-Butyl lithium , *s*-butyl

lithium, and phenyl lithium were purchased from Aldrich as 1-2 M solutions in diethyl ether. *n*-Octyl lithium, *n*-octadecyl lithium, 2-ethyl hexyl lithium and cyclopropyl lithium were prepared from the corresponding alkyl bromide and lithium metal in a procedure similar to that described by Brandsma and Verkruijsse[103] for the preparation of *n*-butyl lithium except that, after the reaction is complete, the solution was filtered through a pad of Celite into a flask equipped with a sidearm stopcock and the volume of the solution was not adjusted. Neopentyl lithium was synthesized as described in the literature,[104] and secondary alkyl lithiums (isopropyl lithium, cyclopentyl lithium) were synthesized in the same manner using the appropriate alkyl chloride.

AlkylCOT derivatives (except for methylCOT) and phenylCOT were synthesized from the appropriate alkyl or aryl lithium, $[n\text{-}Bu_3P{\bullet}CuI]_4$, and bromocyclooctatetraene. A representative procedure for the synthesis of an alkylCOT is as follows: At -30 °C, 230 mL (0.313 moles) of a 0.66 M solution of octyl lithium in diethyl ether was added via cannula with stirring to 60.4 g (39.1 mmol) of $[n\text{-}Bu_3P{\bullet}CuI]_4$ that had been dissolved in ca. 100 mL of diethyl ether. This mixture was stirred for ca. 1 hour. A solution of 7.04 g (39.1 mmol) of bromocyclooctatetraene dissolved in ca 50 mL of diethyl ether was added dropwise. This solution was stirred overnight at -40 °C. The flask was then allowed to warm over the course of ca. 2 hours to -10 °C. Upon reaching this temperature, the flask was cooled to -78 °C and oxygen was bubbled though the solution for 5 minutes. The solution was rewarmed to -10 °C and carefully hydrolyzed with a saturated ammonium chloride solution. The blue aqueous layer was separated from the yellow-green organic layer, washed with diethyl ether and the organics were dried ($MgSO_4$) and concentrated. The organics were collected by Kugelrohr distillation and consisted primarily of the product and R-R (in this case, $n\text{-}C_{16}H_{34}$, GC/MS m/z 226) plus a small amount of residual $n\text{-}Bu_3P$ (GC/MS m/z 202). Pure octylCOT was obtained by distillation (75-85 °C, 0.02 mm) followed by flash chromatography over silica, petroleum ether eluent yielding 5.83 g (70 % based upon moles of bromocyclooctatetraene).

IsopropylCOT was synthesized via the COT dianion as follows: COT (2.1 g, 20 mmol), was dissolved in 100 mL of diethyl ether and cooled to 0 °C. 2.5 g (50 mmol) of isopropyl lithium was transferred to a flask in the drybox and dissolved in 50 mL of diethyl ether and cooled to 0 °C. The solution of isopropyl lithium was added via cannula to the COT solution over the course of approximately 10 minutes. A reddish color indicative of dianion formation was noticed in the flask but did not persist. After the addition was complete, the reaction flask was stirred at 0 °C for 30 minutes. Within the first 10 minutes of this time, the reddish color reappeared. Meanwhile, iodine crystals (4.8 g, 1.5 equiv) were placed into a flask which was evacuated at -196 °C and refilled with argon and warmed. The iodine was then dissolved in 100 mL of diethyl ether. The dianion solution was then added to the iodine solution at 0 °C via cannula. Near the end of the addition, the dark-brown to black solution turned yellow-orange in color. The solution was warmed to room temperature and poured cautiously into water. The layers were separated and the aqueous layer was extracted with fresh diethyl ether. The organic layers were combined, dried ($MgSO_4$), and concentrated. Distillation (49 °C/250 mtorr) sometimes yielded a material that was shown to have a small amount of isopropylcyclooctatriene by GC/MS (*m/z* 148 [parent], 105 [base]). To remove the triene impurity, a mixture of *iso*-propylCOT and *iso*-propylcyclooctatriene (approx 3 g) was added to a slurry of dicyanodichloroquinone (DDQ) in 50 mL of dry benzene. This mixture was stirred under argon at room temperature for 2 hours. The mixture was then poured onto a flash chromatography column and eluted with petroleum ether. The resulting solution was concentrated and redistilled to produce a product that showed little or no triene (< 1 %) by GC/MS (total ion count integration).

***n*-ButylCOT** ^{1}H NMR (400 MHz, $CDCl_3$) δ 5.67 (br, 6H, COT), 5.43 (s, 1H, COT), 1.93 (t, J = 7.0 Hz, COT-CH_2), 1.26 (br, 4H -CH_2CH_2-), 0.79 (t, J = 7.1 Hz, 3H,

-CH_3); $^{13}C\{^1H\}$ NMR (22.5 MHz, $CDCl_3$) δ 144.72, 134.64 (br), 131.85, 131.32 (br), 128.28, 126.13, 37.42, 30.73, 22.22, 13.90; MS *m/z* 160 [parent], 131, 117 [base], 103, 91, 78; *m/e* calcd 160.1252, found 160.1246, Δ = -3.8 ppm.

***n*-OctylCOT** ^1H NMR (500 MHz, $CDCl_3$) δ 5.74 (br, 6H, COT), 5.53 (s, 1H, COT), 2.02 (t, J = 7.4 Hz, 2H, COT-CH_2-), 1.38 (br, 2H), 1.30 (br, 10H, -CH_2-), 0.88 (t, J = 6.8 Hz, 3H, CH_3); $^{13}C\{^1H\}$ NMR (22.5 MHz, $CDCl_3$) δ 144.72, 134.32 (br), 131.85, 131.27 (br), 126.72, 126.07, 37.75, 31.90, 29.43, 29.30, 29.17, 28.52, 22.67, 14.03; MS *m/z* 216 [parent], 187, 159, 131, 117 [base], 103, 91, 78; *m/e* calcd 216.1878, found 216.1870, Δ = -3.7 ppm.

***n*-OctadecylCOT** ^1H NMR (500 MHz, $CDCl_3$) δ 5.74 (br, 6H, COT), 5.53 (s, 1H, COT), 2.02 (t, J = 7.3 Hz, 2H, COT-CH_2), 1.37 (br, 2H), 1.26 (br, 30H, -CH_2-), 0.88 (t, J = 6.8 Hz, 3H, -CH_3); $^{13}C\{^1H\}$ NMR (22.5 MHz, $CDCl_3$) δ 144.72, 134.32 (br), 131.85, 131.33 (br), 126.13 (br), 37.75, 31.97, 29.76, 29.69 (sh), 29.50, 29.37, 29.17, 28.52, 22.67, 14.03; MS *m/z* 357 [parent], 159, 131, 118 [base], 117, 103, 91, 78; *m/e* calcd 356.3443, found 356.3449, Δ = 1.7 ppm.

***s*-ButylCOT** ^1H NMR (500 MHz, $CDCl_3$) δ 5.79 (br, 6H, COT), 5.53 (s, 1H, COT), 2.10 (sex, J = 7.0 Hz, 1H, COT-CH), 1.30 (br, 2H, -CH-CH_2-CH_3), 1.00 (d, J = 7.0 Hz, 3H, -CH-CH_3), 0.87 (br, 3H, -CH_2CH_3); $^{13}C\{^1H\}$ NMR (125 MHz, $CDCl_3$) δ 148.58, 132.33, 131.85, 131.74, 131.59, 131.53, 130.52, 125.26, 43.63, 28.21, 19.84, 12.01; MS *m/z* 160 [parent], 131 [base], 115, 104, 91, 77; *m/e* calcd 160.1252, found

160.1250, Δ = -1.3 ppm. Anal. Calcd. for $C_{12}H_{16}$: C, 89.94; H, 10.06. Found: C, 89.75, H, 9.98.

NeopentylCOT ^{1}H NMR (500 MHZ, $CDCl_3$) δ 5.77 (br, 6H, COT), 5.47 (s, 1H, COT), 1.90 (s, 2H, COT-CH_2), 0.94 (s, 9H, -$C(CH_3)_3$); $^{13}C\{^1H\}$ NMR (125 MHz, $CDCl_3$) δ 142.28, 137.13, 132.34, 132.25, 132.16, 131.30, 130.10, 129.82, 51.89, 31.41, 30.03; MS *m/z* 174 [parent], 159, 143, 129, 117 [base], 103, 91, 78; *m/e* calcd 174.1409, found 174.1404, Δ = -2.6 ppm. Anal. Calcd. for $C_{13}H_{18}$: C, 89.59; H, 10.41. Found: C, 89.29; H, 10.35.

2-EthylhexylCOT Separation by column chromatography of the product from the dimer (5,8-diethyldodecane) was not possible. Purification was effected by preparative gas chromatography on a 15% SE-30 on HP chromasorb column using a column/injector/detector temperatures of 160/210/195 °C respectively (53x50 μL injections). ^{1}H NMR (500 MHZ, $CDCl_3$) δ 5.76 (br, 6H, COT), 5.50 (s, 1H, COT), 1.94 (br, 2H, COT-CH_2), 1.25 (br, 9H, -CH_2- + -CH-), 0.87 (t, J = 6.3 Hz, 3H, -CH_3), 0.82 (t, J = 7.2 Hz, 3H, -CH_3); $^{13}C\{^1H\}$ NMR (22.5 MHz, $CDCl_3$) δ 143.74, 134.77, 131.92, 131.14 (br), 127.43, 42.43, 37.62, 32.36, 28.85, 25.60, 23.06, 14.16, 10.72; MS *m/z* 216 [parent], 187, 159, 131, 117 [base], 103, 91; *m/e* calcd 216.1878, found, 216.1882, Δ = 1.8 ppm.

IsopropylCOT ^{1}H NMR (500 MHZ, $CDCl_3$) δ 5.83 (br, 6H, COT), 5.55 (s, 1H, COT), 2.30 (sep, J = 6.8 Hz, 1H, COT-CH-), 1.03 (d, J = 6.9 Hz, 6H, -CH_3); $^{13}C\{^1H\}$ NMR (22.5 MHz, $CDCl_3$) δ 150.50, 133.02, 131.53 (br), 130.62, 123.47, 33.61 & 35.15

(-CH-, dias.), 22.22, 21.57 (-CH_3, dias.); MS *m/z* 146 [parent], 131 [base], 116, 103; *m/e* calcd 146.1096, found 146.1097, Δ = 1.0 ppm.

CyclopentylCOT ^{1}H NMR (500 MHZ, $CDCl_3$) δ 5.81 (br, 6H, COT), 5.55 (s, 1H, COT), 2.46 (m, 1H, COT-CH-), 1.73 (m, 2H), 1.63 (m, 2H), 1.53 (m, 2H), 1.39 (m, 2H); $^{13}C\{^1H\}$ NMR (22.5 MHz, $CDCl_3$) δ 147.97, 133.34, 132.37, 131.59 (br), 131.01, 130.49, 47.30, 31.71, 25.27; MS *m/z* 172 [parent], 157, 143, 129 [base], 117, 104; *m/e* calcd 172.1252, found 172.1251, Δ = -0.6 ppm.

Polymer Syntheses. The metathesis catalysts, W(CH(*t*-Bu))(N(2,6-(*i*-Pr)$_2$C$_6$H$_3$)-(OCMe(CF$_3$)$_2$)$_2$, (2)[36] and W(CH(*o*-MeOPh))(NPh)(OCMe(CF$_3$)$_2$)$_2$•THF, (3)[37] were prepared using literature methods. Polymerizations and subsequent handling of polymer films and preparation of polymer solutions were conducted in a nitrogen-filled Vacuum Atmospheres drybox. In a typical polymerization, 2-3 mg of catalyst (2 or 3) were weighed into a tared vial and dissolved in a minimum of pentane (2-3 drops). One drop of THF was added to catalyst 2 to slow the rate of polymerization. Lewis bases will reversibly bind to the catalyst, slowing the rate of propagation considerably.[77] Catalyst 3 already has a molecule of THF precoordinated to the metal center. To this mixture, 150 ± 10 molar equivalents (≈ 150-250 μL depending on the monomer employed) of monomer (in all cases described here, a yellow liquid) was added, and the contents of the vial were mixed. The mixture typically began to turn a darker orange-brown color within 15 seconds, signifying the onset of polymerization. Over the next minute or so, the mixture could be transferred by pipette to a glass slide or other non-interacting substrate such as a KBr die or polyethylene film. Here, the mixture hardened into a dark film which could then be removed from the substrate with a razor blade. To specifically terminate the

polymerization, the polymer was dissolved and 50 equivalents of benzaldehyde or isovaleraldehyde were added immediately. Samples could then be filtered for study by NMR or GPC. Alternatively, films were rinsed repeatedly at 0 °C with dry pentane and methanol under argon in order to remove soluble components such as residual monomer, catalyst decomposition products, and substituted benzene produced by back-biting during the polymerization. After rinsing, the films were subjected to dynamic vacuum to remove solvent until a vacuum of < 1 mtorr was achieved. By rinsing at low temperature and protecting the films from light, the highest possible cis content was insured.

Cis/trans isomerization. Isomerization of the polymer from a predominantly cis configuration to a predominantly trans configuration could be accomplished either thermally or photochemically. Thermal isomerization was accomplished by heating the sample in benzene or THF at 60-80 °C in a tube sealed with a teflon Kontes screw top until the visible absorption spectrum showed no change. Photochemical isomerization was accomplished at 0 °C (monitored by thermocouple and external meter in the bath) by exposure of the sample dissolved in THF or benzene to light from a Pyrex-filtered, 350 watt, medium pressure mercury Hanovia lamp (approx 6-12 hours for a ≈ 1 mg/mL sample). Overexposure resulted in a decrease in color indicating decomposition of the material in solution. THF, toluene and benzene were suitable solvents for this experiment. Chlorinated solvents sometimes lead to photobleaching.

Isomerized solutions could be recast into films that were shiny and green-gold in color. Although isomerization rendered many polymers almost completely insoluble, the inhomogeneous partially precipitated suspensions that resulted from isomerization of poly-neopentylCOT were recast into shiny green-gold films, allowing for investigation of some of the properties of completely isomerized insoluble material.

Kinetic Measurements on *trans*-poly-*s*-butylCOT. Rates for cis/trans isomerization of poly-*s*-butylCOT were determined by observing the rate of appearance

of the peak at 560 nm of a 4×10^{-5} M solution of the polymer in either THF or benzene. Temperature was controlled via a constant temperature bath (error ± 2 °C). Construction of Arrhenius and Eyring plots and subsequent determination of $\Delta H^{\ddagger}$ and $\Delta S^{\ddagger}$ are described in the literature.[105] Magnetization transfer was accomplished using a 180_A-τ-90_B pulse sequence at 50 °C in C_6D_6 as described in the literature.[106] The resonance at 2.5 ppm (A) was irradiated and both this resonance and the resonance at 2.8 ppm (B) were integrated. An ethylene glycol temperature standard was used to calibrate the probe temperature (error ± 1 °C). T_1 values were obtained using a standard inversion recovery sequence (180_A-τ-90_A).

Calculation of %Conversion and %Backbiting by NMR. Figure 16 shows the olefinic region of the ^1H NMR spectrum of the product of a typical polymerization. This spectrum is of the predominantly cis form of the polymer in the mixture, and although the shape of the olefinic polymer peak changes during isomerization to the predominantly trans form, it does not change the calculation shown here. The olefin region here is similar for any soluble polyacetylene derivative reaction mixture, and the calculation of percent conversion and percent cycloextrusion is performed in an identical manner for all polymers.

One can identify three resolved integrals in Figure 15 ~~16~~: I_1, I_2, and I_3. They are the integration of the following:

I_1: Cycloextrusion product (5H). We do not consider the contribution by the phenyl imido group in the catalyst or the ortho-methoxy benzylidene group on the tail of the polymer which also displays resonances in this region. Thus we get a higher estimate of percent cycloextrusion.

I_2: Integration of all protons on the polymer backbone plus six protons of the residual monomer (sharp peaks upfield).

I_3: One proton of the residual monomer, based on comparison with the ^1H NMR spectrum of the monomer.

We define three variables:

X = moles of unreacted monomer

Y = moles of monomer that reacted with the catalyst

Z = moles of cycloextrusion product.

Thus the polymers in this study are effectively copolymers of the repeat units shown in Figure 16. In this figure, repeat units are shown in the all-*trans* form. The isomeric content of the polymers is irrelevant for the calculations shown here.

Now, we can express the three integrals in terms of X, Y, and Z:

$$I_1 = 5Z \qquad I_2 = 6X + (7Y - 5Z) \qquad I_3 = X$$

In the treatment above, the quantity 7Y - 5Z is all the olefin protons in the polymer, i.e. all the olefin protons in the monomer minus those lost to cycloextrusion product.

Given I_1, I_2, and I_3, we can solve for X, Y, and Z. Then,

$$\% \text{ conversion} = \frac{Y}{Y+X}$$

$$\% \text{ backbiting} = \frac{Z}{Y}$$

Instrumentation. Ultraviolet-visible absorption spectroscopy was performed on either an HP 8451A or an HP 8452A diode array spectrophotometer. Low temperature optical spectra were obtained by placing a solution in an NMR tube into the window of a clear quartz finger Dewar flask filled with a dry ice/acetone slurry. Absorption spectra in the near infrared were collected on a Cary 14 UV/VIS/NIR modified by online instruments. Gel permeation chromatography was performed on one of two instruments: a homemade instrument employing three Shodex size exclusion columns, model numbers KF-803, KF-804, and KF-805 (70,000, 400,000, and 4,000,000 MW polystyrene exclusion limit, respectively), an Altex model 110A pump and a Knauer differential refractometer and a Kratos UV detector (detection at the visible absorption maximum of the polymer sample), with CH_2Cl_2 as an eluant at a flow rate of 1.5 mL/min, or a Waters GPC-150C with THF as an eluant. Molecular weights are reported relative to narrow molecular weight polystyrene standards. GPC samples (0.5 wt%) were filtered through a 0.5 μm filter prior to injection. Static light scattering data were obtained by Glen Heffner and Dale Pearson (UC Santa Barbara). Resonance Raman spectra were obtained using 488 nm excitation from an argon ion laser source using two different setups. The first employed a SPEX monochromator, a power source of 300-330 mW, and each sample was referenced to the known absorption frequencies of a CCl_4 or silicon sample. Data on the second apparatus was collected by Hyun Chae Cynn and Dr. Malcom Nicol at UC Los Angeles employing a Princeton Instrument IRY 1024/G optical multichannel analyzer that was sensitive enough to permit employment of a much lower incident power (≈ 50 mW). In this setup, the wavelength scale of the detector was calibrated using

diamond and calcite samples. In both cases, samples were polymer films enveloped between two thin glass plates (biological cover slips) or were polymer films on a single glass substrate. It was found that scattering the light directly off of the polymer films gave consistently higher signal to noise ratios. No attempt was made to cool the sample during analysis.

Scanning electron microscopy of gold-coated samples (10 nm coating, sputtered deposition) was performed using 20 KeV electrons (micrographs taken in back-scattering mode). X-ray diffraction was measured by wide angle scattering from a Guinier camera employing monochromatic Cu K_α radiation. Thermal analysis was performed under a nitrogen purge on a Perkin Elmer DSC-7 differential scanning calorimeter and a Perkin Elmer TGS-2 thermogravimetric analyzer both at a scanning rate of 20 °C/min.

Doping and Conductivity measurements. Doping was accomplished by exposing the polymer films to iodine vapor for 3 to 6 hours in a previously evacuated chamber followed by pumping (< 0.01 torr) for approximately one hour or longer to remove any excess iodine. Films immediately became blue-black in color but generally remained flexible. A profile of iodine concentration obtained by energy dispersive spectroscopy (EDS) through a cross section of films showed that iodine was homogeneously distributed throughout them. Conductivities were measured using a four-point probe in a nitrogen drybox or a four-wire probe attached to a Schlenk line.[107] Similar conductivities were observed using both methods. Film thicknesses were measured either with Fowler Digitrix II digital calipers or a Dektak 3030a profilometer. A JEOL 733 electron microprobe equipped with wavelength-dispersive X-ray detectors was used for energy dispersive spectroscopy (EDS).

Doping in solution. A solution of *trans*-poly-*s*-butylCOT was doped with $NOPF_6$ as was reported for solution-doped poly-alkylthiophenes.[71] The appropriate amount of a 4 mg/mL solution of $NOPF_6$ in CH_3CN was added to a 2 mg/mL solution of

trans-poly-*s*-butylCOT in $CHCl_3$ to give doping levels between y = 0.05 and y = 0.20 ($(C_{12}H_{16})(NOPF_6)_y$). Solutions were observed to decompose (e.g. turn from deep blue to brown in color) over the course of 5-10 minutes at room temperature but were stable over the course of weeks at -50 °C under inert atmosphere.

Computations. Geometry optimizations of model oligomers **5** and **6** were performed using the MM2 force field available in Batchmin[108] Version 3.1b (on a DEC MicroVax 3500) or Version 2.6 (on a Silicon Graphics Iris 4D/220GTX workstation). The derivatives convergence criterion was employed, with convergence defined to be when the root mean square of the first derivative reached 0.1. Both the global and several local conformational minima were discovered using Monte Carlo methods. In this method, a number of conformations are generated and then minimized to find structures corresponding to local minima in the potential energy surface.[94] This method was employed to insure that the optimized geometries corresponded to a global minimum.

Geometry optimization of the same models was obtained at the semiempirical level using the AM1 parameterization in AMPAC version 1.00[52] on a DEC MicroVax 3500. Molecular dynamics calculations[94] were run using the MM2 force field at 300 K for 20 ps using Batchmin.[108] Torsions around Θ_1 and Θ_2 were monitored using the MDDA option.

Acknowledgments

This research was supported by the Office of Naval Research. For research fellowship support, CBG thanks the NASA Jet Propulsion Laboratory and the American Chemical Society Division of Organic Chemistry (Sponsored by SmithKline & French Laboratories). EJG also thanks IBM for a research fellowship. We thank BASF for a gift of cyclooctatetraene. We thank Bruce Tiemann and Maie Abdulrahman for technical

assistance, Glenn Heffner and Prof. Dale Pearson at the University of California, Santa Barbara for light scattering data, Hyun Chae Cynn and Prof. Malcom Nicol at the University of California, Los Angeles for some of the Raman spectra, Lynda Johnson for the preparation and generous gift of catalyst **3** and Scott Virgil for preparation of catalyst precursors for **2**. We thank Prof. Greg Baker and Prof. Pierre-Gilles DeGennes for informative discussions on polymer solubility.

References

(1) Patil, A. O.; Heeger, A. J.; Wudl, F. *Chem. Rev.* **1988**, *88*, 183-200.

(2) Kajzar, F.; Etemad, S.; Baker, G. L.; Messier, J. *Synth. Met.* **1987**, *17*, 563-567.

(3) Chemla, D. S.; Zyss, J., Ed. *Nonlinear Optical Properties of Organic Materials and Crystals, Vols. 1 & 2*. Academic: Orlando, FL, 1987.

(4) Marder, S. R.; Sohn, J. E.; Stucky, G. D., Ed. *Materials for Nonlinear Optics: Chemical Perspectives*. American Chemical Society, Symposium Series Vol. 455; American Chemical Society: Washington, 1991.

(5) Skotheim, T. A., Ed. *Handbook of Conducting Polymers*. Vol. 1 and 2; Marcel Dekker: New York, 1986.

(6) Gorman, C. B.; Grubbs, R. H. In *Conjugated Polymers: The Novel Science and Technology of Conducting and Nonlinear Optically Active Materials*; Brédas, J. L.; Silbey, R. Ed.; Kluwer Academic Publishers: Dordrecht, The Netherlands, 1992; pp 1-48.

(7) Brandstetter, F. *ECN Speciality Chemicals Supp.* **1988**, *Jan.*, 32-36.

(8) Freundlich, N. *Business Week* **1989**, *Dec. 11*, 114-5.

(9) Frommer, J. E.; Chance, R. R. In *Encyclopedia of Polymer Science and Engineering*; Ed.; Vol. 5; Wiley & Sons: 1986; pp 462-507.

(10) Sailor, M. J.; Ginsburg, E. J.; Gorman, C. B.; Kumar, A.; Grubbs, R. H.; Lewis, N. S. *Science* **1990**, *249*, 1146-1149.

(11) Wilson, J.; Hawkes, J. F. B. *Optoelectronics: An introduction, 2nd ed.*; Prentice Hall: New York, 1989, pp 470.

(12) Hotta, S.; Rughooputh, S. D. D. V.; Heeger, A. J.; Wudl, F. *Macromolecules* **1987**, *20*, 212-215.

(13) Rughooputh, S. D. D. V.; Hotta, S.; Nowak, M.; Heeger, A. J.; Wudl, F. *Synth. Met.* **1987**, *21*, 41-50.

(14) Jen, K. Y.; Oboodi, R. L.; Elsenbaumer, R. L. *Polym. Mat. Sci. Eng.* **1985**, *53*, 79-83.

(15) Cis/trans content has been probed for some polyacetylene derivatives, and it appears that bulkier side groups increase the cis content of the polymer: Leclerc, M.; Prud'homme, R. E.; Soum, A.; Fontanille, M. *J. Polym. Sci. Polym. Phys. Ed.* **1985**, *23*, 2031-2041.

(16) MacIness Jr., D.; Funt, B. L. *Synth. Met.* **1988**, *25*, 235-242.

(17) Elsenbaumer, R. L.; Jen, K.; Miller, G. G.; Eckhardt, H.; Shacklette, L. W.; Jow, R. In *Electronic Properties of Conjugated Polymers.*; Kuzmany, H.; Mehring, M.; Roth, S. Ed.; Vol. 76; Springer-Verlag: Berlin, 1987; pp 400-406.

(18) Rehahn, M.; Schlüter, A. D.; Wegner, G.; Feast, W. J. *Polymer* **1989**, *30*, 1054-1059.

(19) Rehahn, M.; Schlüter, A. D.; Wegner, G.; Feast, W. J. *Polymer* **1989**, *30*, 1060-1062.

(20) Ballauff, M. *Angew. Chem. Int. Ed. Engl.* **1989**, *28*, 253-267.

(21) This issue is not straightforward since long alkyl side chains can themselves crystallize: Rabolt, J. F.; Hofer, D.; Fickes, G. N.; Miller, R. D. *Macromolecules* **1986**, *19*, 611-6.

(22) Masuda, T.; Higashimura, T. *Adv. Polym. Sci.* **1986**, *81*, 121-165.

(23) Masuda, T.; Higashimura, T. *Acc. Chem. Res.* **1984**, *17*, 51-56.

(24) Gibson, H. W. In *Handbook of Conducting Polymers, Vol. 1*; Skotheim, T. Ed.; Marcel Dekker: New York, 1986; pp 405-439.

(25) Furlani, A.; Napoletano, C.; Paolesse, R.; Russo, M. V. *Synth. Met.* **1987**, *21*, 337-342.

(26) Petit, M. A.; Soum, A. H.; Leclerc, M.; Prud'homme, R. E. *J. Polym. Sci. Polym. Phys.* **1987**, *25*, 423-433.

(27) Leclerc, M.; Prud'homme, R. E. *Macromolecules* **1987**, *20*, 2153-2159.

(28) Brédas, J. L.; Heeger, A. J. *Macromolecules* **1990**, *23*, 1150-1156.

(29) Gorman, C. B.; Ginsburg, E. J.; Marder, S. R.; Grubbs, R. H. *Angew. Chem. Adv. Mater.* **1989**, *101*, 1603-1606.

(30) Ginsburg, E. J.; Gorman, C. B.; Marder, S. R.; Grubbs, R. H. *J. Am. Chem. Soc.* **1989**, *111*, 7621-7622.

(31) Ivin, K. J. *Olefin Metathesis*; Academic: London, 1983.

(32) Grubbs, R. H. In *Comprehensive Organometallic Chemistry*; Wilkinson, G. Ed.; Vol. 8; Pergamon: New York, 1982; pp 499-551.

(33) Korshak, Y. V.; Korshak, V. V.; Kanischka, G.; Höcker, H. *Makromol. Chem., Rapid Commun.* **1985**, *6*, 685-692.

(34) Tlenkopachev, M. A.; Korshak, Y. V.; Orlov, A. V.; Korshak, V. V. *Doklad. Akad. Nauk, Eng. Transl.* **1987**, *291*, 1036-1040 (Original Russian article: pp. 409-413, 1986).

(35) Klavetter, F. L.; Grubbs, R. H. *J. Am. Chem. Soc.* **1988**, *110*, 7807-7813.

(36) Schrock, R. R.; DePue, R. T.; Feldman, J.; Schaverien, C. J.; Dewan, J. C.; Liu, A. H. *J. Am. Chem. Soc.* **1988**, *110*, 1423-1435.

(37) Johnson, L. K.; Virgil, S. C.; Grubbs, R. H. *J. Am. Chem. Soc.* **1990**, *112*, 5384-5385.

(38) Kuzmany, H. *Pure and Appl. Chem.* **1985**, *57*, 235-246.

(39) Gibson, H. W.; Kaplan, S.; Mosher, R. A.; W. M. Prest, J.; Weagley, R. J. *J. Am. Chem. Soc.* **1986**, *108*, 6843-6851.

(40) Ito, T.; Shirakawa, H.; Ikeda, S. *J. Polym. Sci. Polym. Chem. Ed.* **1975**, *13*, 1943.

(41) Gibson, H. W.; Weagley, R. J.; Mosher, R. A.; Kaplan, S.; Prest, J., W. M.; Epstein, A. J. *Phys. Rev. B.* **1985**, *31*, 2338-2342.

(42) Kohler, B. E. *J. Chem. Phys.* **1988**, *88*, 2788-2792.

(43) Robin, P.; Pouget, J. P.; Comés, R.; Gibson, H. W.; Epstein, A. J. *Journal de Physique* **1983**, *44*, C3-77.

(44) Hoffman, D. M.; Gibson, H. W.; Epstein, A. J.; Tanner, D. B. *Phys. Rev. B.* **1983**, *27*, 1454-1457.

(45) Francois, B.; Bernard, M.; Andre, J. J. *J. Chem. Phys.* **1981**, *75*, 4142-4152.

(46) Tanaka, M.; Yasuda, H.; Tanaka, J. *Bull. Chem. Soc. Jpn.* **1982**, *55*, 3639-3640.

(47) Kohler, B. E.; Mitra, P.; West, P. *J. Chem. Phys.* **1986**, *85*, 4436-4440.

(48) Ohmine, I.; Morokuma, K. *J. Chem. Phys.* **1981**, *74*, 564-569.

(49) Sandros, K.; Sundahl, M.; Wennerström, O.; Norinder, U. *J. Am. Chem. Soc.* **1990**, *112*, 3082-3086.

(50) Oki, M. *Applications of Dynamic NMR Spectroscopy to Organic Chemistry*; Methods in Stereochemical Analysis Vol. 4; VCH Publishers: Deerfield Beach, Florida, 1985, pp 106-139.

(51) Doering, W. v. E.; Kitagawa, T. *J. Am. Chem. Soc.* **1991**, *113*, 4288-4297.

(52) Dewar, M. J. S.; Zoebisch, E. G.; Healy, E. F.; Stewart, J. J. P. *J. Am. Chem. Soc.* **1985**, *107*, 3902-3909.

(53) Kolev, V. D. *J. Mol. Struct.* **1984**, *114*, 257-260.

(54) Schaffer, H. E.; Chance, R. R.; Knoll, K.; Schrock, R. R.; Silbey, R. In *Conjugated Polymeric Materials: Opportunities in Electronics, Optoelectronics, and Molecular Electronics*; Bredas, J. L.; Chance, R. R. Ed.; NATO ASI Series. Series E: Applied Sciences Vol. 182; Kluwer Academic Publishers: Dordrecht, The Netherlands, 1990; pp 365-376.

(55) Moses, D.; Feldblum, A.; Ehrenfreund, E.; Heeger, A. J.; Chung, T.-C.; MacDiarmid, A. G. *Phys. Rev. B.* **1982**, *26*, 3361-3369.

(56) Sklar, L. A.; Hudson, B. S.; Petersen, M.; Diamond, J. *Biochemistry* **1977**, *16*, 813-819.

(57) Bohlmann, F. *Chem. Ber.* **1952**, *85*, 386-389.

(58) Bohlmann, F. *Chem. Ber.* **1953**, *86*, 63-69.

(59) Bohlmann, F.; Kieslich, K. *Chem. Ber.* **1954**, *87*, 1363-1372.

(60) Nayler, P.; Whiting, M. C. *J. Chem. Soc. Chem. Comm.* **1955**, 3037-3046.

(61) Sondheimer, F.; Ben-Efraim, D. A.; Wolovsky, R. *J. Am. Chem. Soc.* **1961**, *83*, 1675-1681.

(62) Karrer, P.; Eugster, C. H. *Helv. Chim. Acta* **1951**, *34*, 1805-1814.

(63) D'Amico, K. L.; Manos, C.; Christensen, R. L. *J. Am. Chem. Soc.* **1980**, *102*, 1777-1782.

(64) Winston, A.; Wichacheewa, P. *Macromolecules* **1973**, *6*, 200-205.

(65) Kohler, B. E. In *Electronic Properties of Polymers and Related Compounds*; Kuzmany, H.; Mehring, M.; Roth, S. Ed.; Springer Ser. Solid State Sci. Vol. 63; Springer-Verlag: New York, 1985; pp 100-106.

(66) Kohler, B. E.; Pescatore, J., J. A. In *Conjugated Polymeric Materials: Opportunities in Electronics, Optoelectronics, and Molecular Electronics*; Bredas, J. L.; Chance, R. R. Ed.; NATO ASI Series. Series E: Applied Sciences Vol. 182; Kluwer Academic Publishers: Dordrecht, The Netherlands, 1990; pp 353-364.

(67) For a review of polyene spectroscopy, see: Hudson, B.; Kohler, B. E. *Synth. Met.* **1984**, *9*, 241-253.

(68) Kohler, B. E. Personal Communication

(69) Knoll, K.; Schrock, R. R. *J. Am. Chem. Soc.* **1989**, *111*, 7989-8004.

(70) This is based upon the Fieser-Kuhn rules for polyene optical spectra. For a description, see: Silverstein, R. M.; Bassler, G. C.; Morrill, T. C. *Spectrometric Identification of Organic Compounds, Fourth Ed.*; John Wiley & Sons: New York, 1981, Chapter 6.

(71) Nowak, M. J.; Rughooputh, S. D. D. V.; Hotta, S.; Heeger, A. J. *Macromolecules* **1987**, *20*, 965-968.

(72) Jozefiak, T. H.; Gorman, C. B.; Ginsburg, E. J.; Lewis, N. S.; Grubbs, R. H. Submitted.

(73) Kitching, W.; Olszowy, H.; Drew, G. M.; Adcock, W. *J. Org. Chem.* **1982**, *47*, 5133-5156.

(74) de Melo, C. P.; Silbey, R. *J. Chem. Phys.* **1988**, *88*, 2558-2566.

(75) Soos, Z. G.; Hayden, G. W. *Phys. Rev. B.* **1989**, *40*, 3081-3089.

(76) DeGennes, P. J. Personal communication

(77) Klavetter, F. L.; Ph. D. Dissertation; California Institute of Technology: 1989.

(78) A vast number of approaches that have been taken, and the reader is referred to a review: Stowell, J. A.; Amass, A. J.; Beevers, M. S.; Farren, T. R. *Polymer* **1989**, *30*, 195-201.

(79) Tubino, R.; Dorsinville, R.; Lam, W.; Alfano, R. R.; Birman, J. L.; Bolognesi, A.; Destri, S.; Catellani, M.; Porzio, W. *Phys. Rev. B* **1984**, *30*, 6601-6605.

(80) Piaggio, P.; Cuniberti, C.; Dellepiane, G.; Bolognesi, A.; Catellani, M.; Destri, S.; Porzio, W.; Tubino, R. *Synth. Met.* **1987**, *17*, 337-342.

(81) Dorsinville, R.; Yang, L.; Alfano, R. R.; Tubino, R.; Destri, S. *Solid State Commun.* **1988**, *68*, 875-877.

(82) Pfleger, J.; Kminek, I.; Nespurek, S.; Prasad, P. N. *Synth. Met.* **1990**, *37*, 255-261.

(83) Dorsinville, R.; Tubino, R.; Krimchansky, S.; Alfano, R. R.; Birman, J. L.; Bolognesi, A.; Destri, S.; Castellani, M.; Porzio, W. *Phys. Rev. B* **1985**, *32*, 3377-3380.

(84) VanNice, F. L.; Bates, F. S.; Baker, G. L.; Carroll, P. J.; Patterson, G. D. *Macromolecules* **1984**, *17*, 2626-2629.

(85) Krouse, S. A.; Schrock, R. R. *Macromolecules* **1988**, *21*, 1885-1888.

(86) Weinberger, B. R.; Roxlo, C. B.; Etemad, S.; Baker, G. L.; Orenstein, J. *Phys. Rev. Lett.* **1984**, *53*, 86-89.

(87) Grubbs, R. H.; Gorman, C. B.; Ginsburg, E. J.; Perry, J. W.; Marder, S. R. In *Materials for Nonlinear Optics: Chemical Perspectives*; Marder, S. R.; Sohn, J. E.; Stucky, G. D. Ed.; ACS Symposium Series Vol. 455; American Chemical Society: Washington, DC, 1991; pp 672-682.

(88) Edwards, J. H.; Feast, W. J.; Bott, D. C. *Polymer* **1984**, *25*, 395-398.

(89) Bott, D. C. *Polym. Prepr.* **1984**, *25*, 219-220.

(90) Chien, J. C. W. *Polyacetylene: Chemistry, Physics, and Material Science*; Academic: Orlando, FL, 1984, pp 634.

(91) Kao, J.; Allinger, N. L. *J. Am. Chem. Soc.* **1977**, *99*, 975-986.

(92) MM2 employs a Lennard-Jones potential of the form $E = a/r^6 + b/r^{12}$.

(93) Cernia, E.; D'ilario, L. *J. Polym. Sci. Polym. Chem. Ed.* **1983**, *21*, 2163-2176.

(94) Gunsteren, W. F. v.; Berendsen, H. J. C. *Angew. Chem. Int. Ed. Engl.* **1990**, *29*, 992-1023.

(95) Ryckaert, J. P.; Ciccotti, G.; Berendsen, H. J. C. *J. Comp. Phys.* **1977**, *23*, 327-341.

(96) Still, W. C.; Kahn, M.; Mitra, A. L. *J. Org. Chem.* **1978**, *43*, 2923-2925.

(97) Gasteiger, J.; Gream, G.; Huisgen, R.; Konz, W.; Schnegg, U. *Chem. Ber.* **1971**, *104*, 2412-2419.

(98) Kauffman, G. B.; Teter, L. A. *Inorg. Synth.* **1963**, *7*, 10-11.

(99) Oth, J. F. M.; Merényi, R.; Martini, T.; Schröder, G. *Tet. Lett.* **1966**, 3087-3093.

(100) Harmon, C. A.; Streitweiser, A., Jr. *J. Org. Chem.* **1973**, *38*, 549-551.

(101) Cooke, M.; Russ, C. R.; Stone, F. G. A. *J. C. Dalton* **1975**, 256-259.

(102) Alternate conditions were reported for the synthesis of *t*-butylCOT: Miller, M. J.; Lyttle, M. H.; Streitwieser Jr., A. *J. Org. Chem.* **1981**, *46*, 1977-1984.

(103) Brandsma, L.; Verkruijsse, H. *Preparative Polar Organometallic Chemistry*; Springer-Verlag: New York, 1987, pp 17-18.

(104) Schrock, R. R.; Feldman, J. D. *J. Am. Chem. Soc.* **1978**, *100*, 3359.

(105) Sandström, J. *Dynamic NMR Spectroscopy*; Academic Press: San Diego, 1982.

(106) Mann, B. E. In *Annual Reports on NMR Spectroscopy*; Webb, G. A. Ed.; Vol. 12; Academic Press: San Diego, 1982; pp 272.

(107) Sze, S. M. *Physics of Semiconductor Devices*; Wiley & Sons: New York, 1981, pp 30.

(108) Still, W. C. Columbia University, 1990.

Captions of Figures, Tables and Schemes

Figure 1. Steric repulsions in (a) polymers of substituted acetylenes, (b) polymers of substituted cyclooctatetraenes.

Figure 2. ^{1}H NMR spectra of (bottom) isopropylCOT, (middle) *cis*-poly-isopropylCOT, (top) *trans*-poly-isopropylCOT.

Figure 3. Typical Raman spectrum of *trans*-poly-RCOT.

Figure 4. Thermal cis/trans isomerization of poly-*s*-butylCOT in benzene solution.

Figure 5. Kinetics of thermal of cis/trans isomerization of poly-*s*-butylCOT at 65 °C in benzene, monitored by absorbance at 560 nm.

Figure 6. A ^{1}H NMR spectrum of the methine region of the side groups in partially isomerized poly-s-butylCOT reveals a total of three species. These are assigned to cis/cis (cc), cis/trans (ct) and trans/trans (tt) diads as indicated above. The upfield multiplet at 1.93 ppm is due to residual monomer.

Figure 7. Model tetraenes used to determine heats of formation as a function of side group and isomeric composition.

Figure 8. Relative heats of formation of various isomers of 4 for various side groups (AM1).

Figure 9. Absorption spectrum for *cis*- and *trans*-poly-*s*-butylCOT in THF. The absorption of the cis polymer is blue shifted compared to the trans polymer as is observed for polyacetylene.

Figure 10. Optical absorption maxima of trans-copolymers in THF as a function of comonomer feed ratio. Polymers possessing an optical absorption maximum beyond approximately 580 nm are insoluble.

Figure 11. Model compounds **5** and **6** used for MM2 and AM1 computations.

Figure 12. Model compound **5** showing the dihedral angles that twist when the geometry is optimized. The same angles are reported for compound **6**.

Figure 13. Graphical representations of twist angles for different side groups in model compound **5** (MM2 results, C3 = cyclopropyl, Np = neopentyl).

Figure 14. Values of torsion angle Θ_1 at 10 fs intervals accumulated during a 20 ps molecular dynamics run at 300 K (Batchmin, MM2) for **5**.[108]

Figure ~~15~~ 16. Repeat units contained in the polymers.

Figure ~~16~~ 15. Typical ^1H NMR ($CDCl_3$) of the olefinic region of poly-R-COT.

Table 1. Molecular weights (GPC) of the cis polymers

Table 2. Differences in the heat of formation of isomers of **4**.

Table 3. Visible absorption, Raman, electrical conductivity and differential scanning calorimetry data for poly-RCOT's.

Table 4. Computed twist angles for model compounds **5** and **6**.

Scheme 1. Polymer synthesis via the ring-opening metathesis polymerization (ROMP) of monosubstituted cyclooctatetraene (COT) derivatives.

Scheme 2. Cycloextrusion of an aromatic compound during COT polymerization.

Figure 1

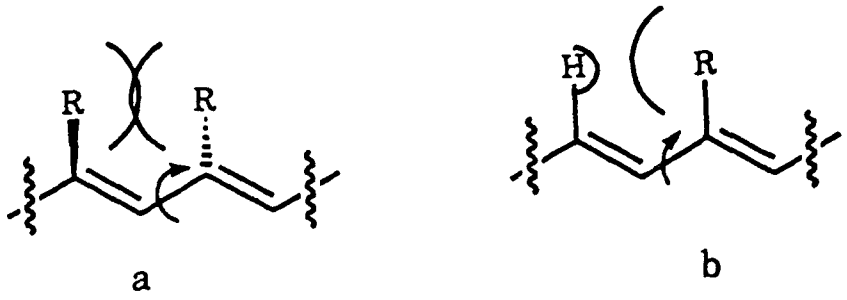

a b

Figure 2

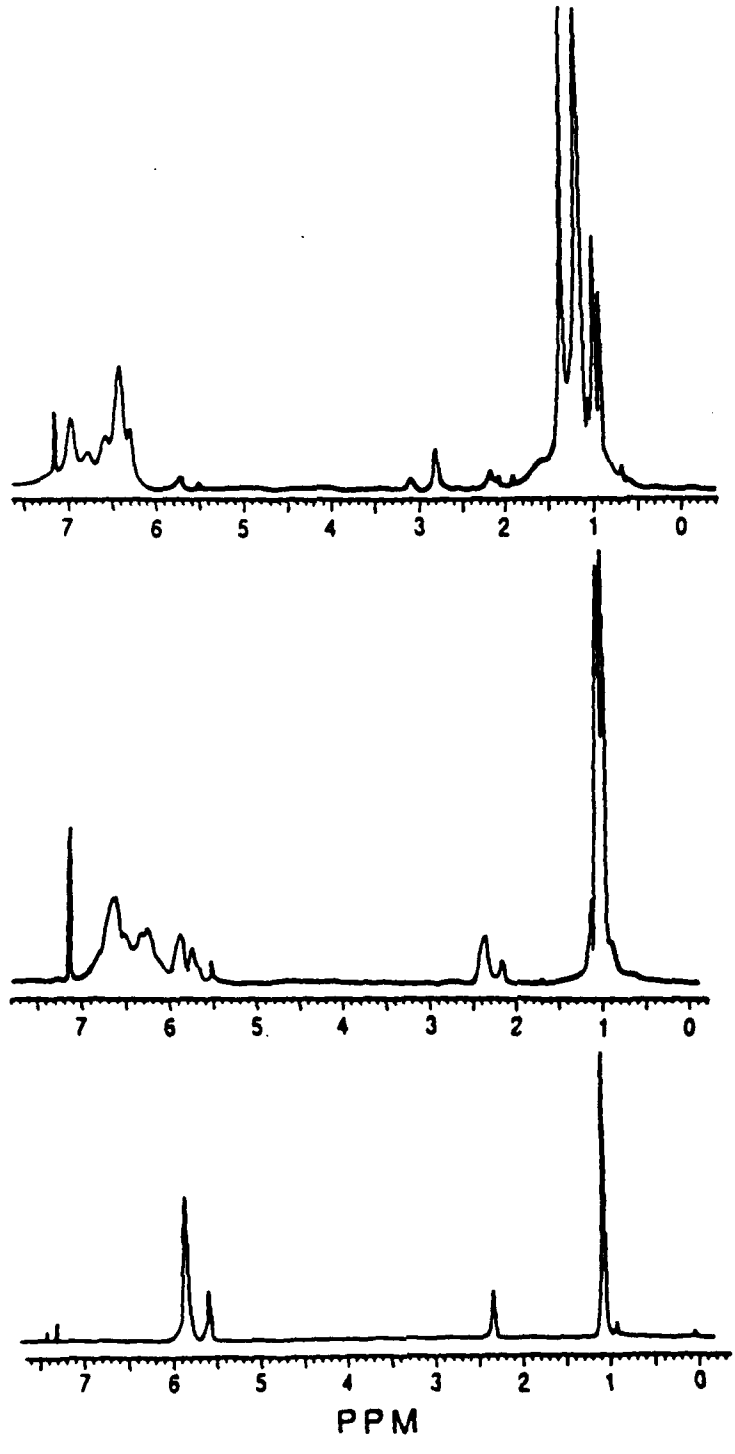

Figure 3

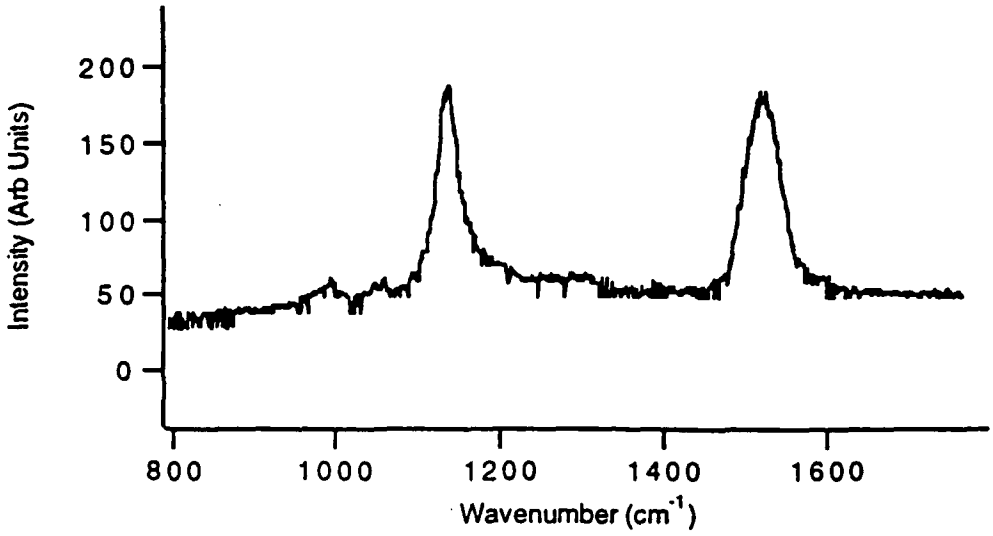

Figure 4

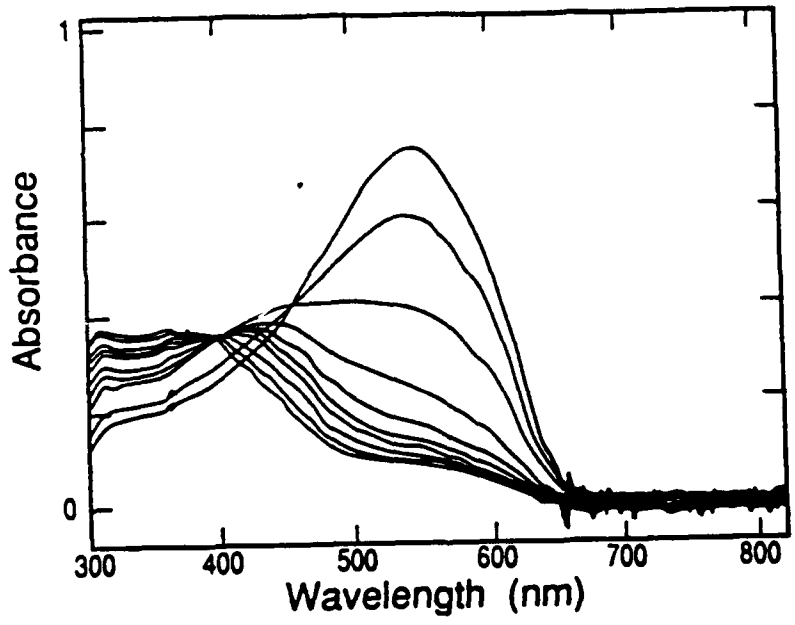

Figure 5

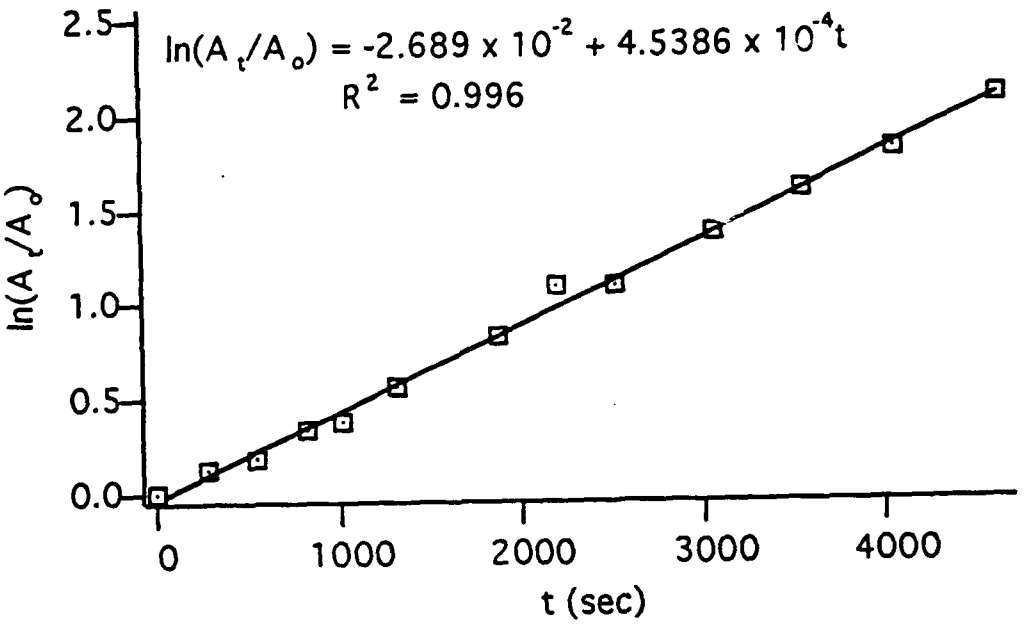

Figure 6

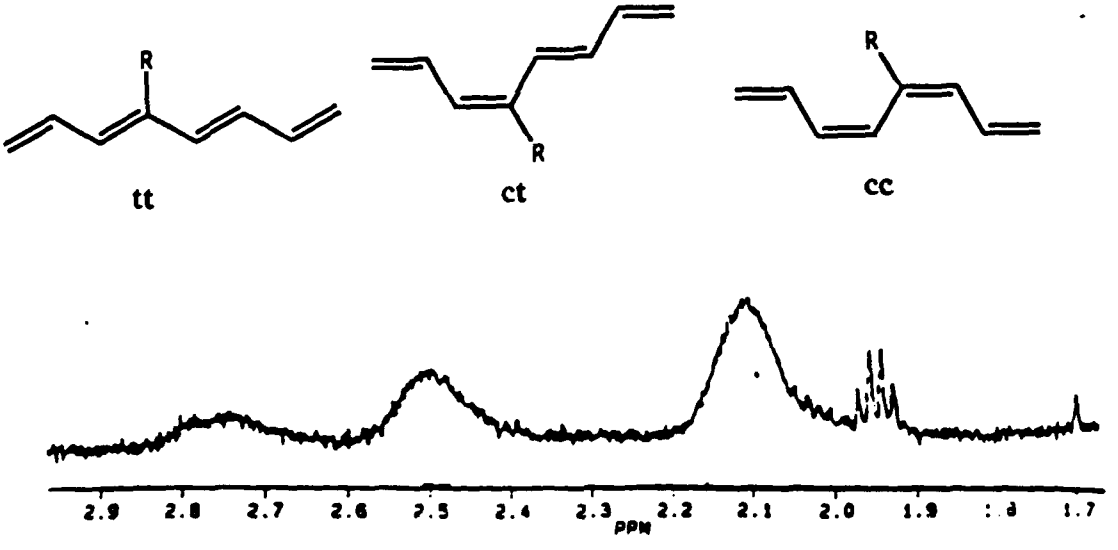

Figure 7

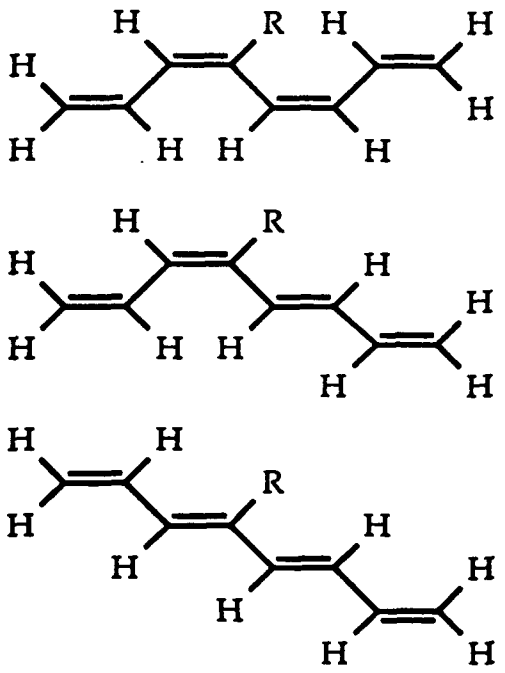

Figure 8

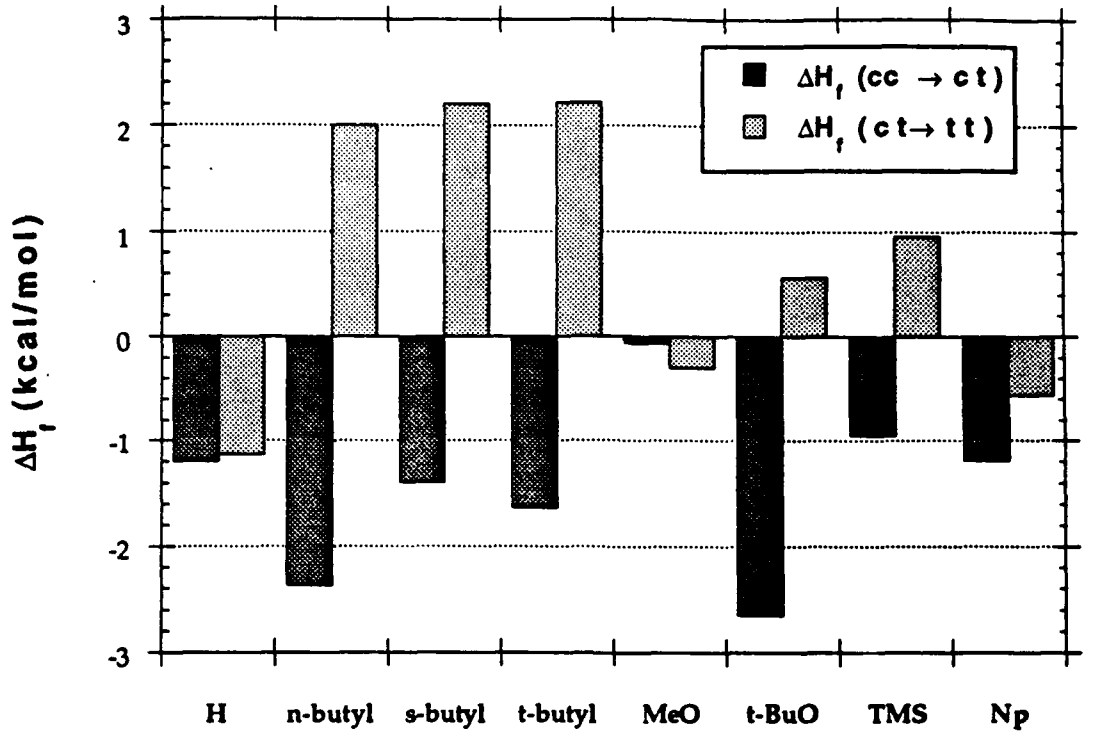

Figure 9

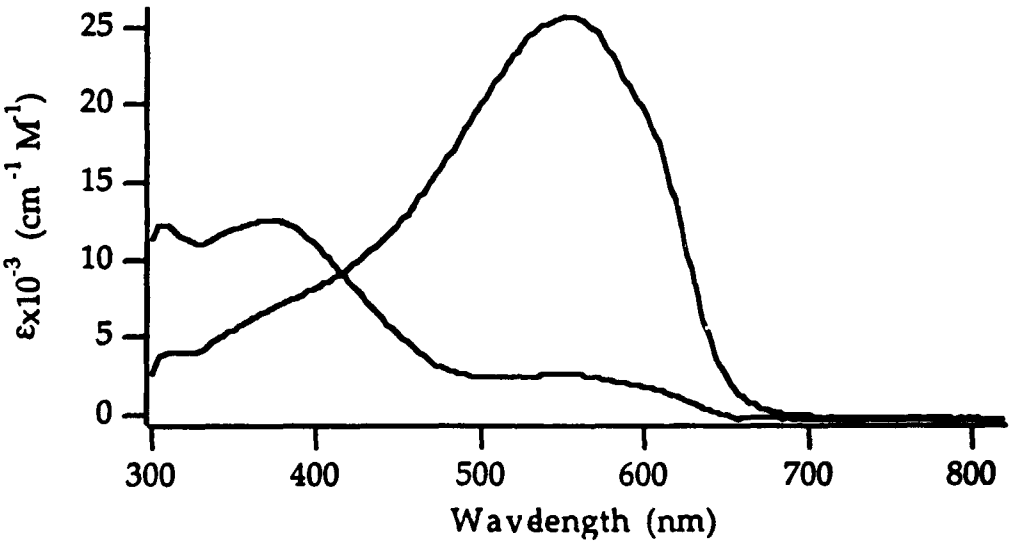

Figure 10

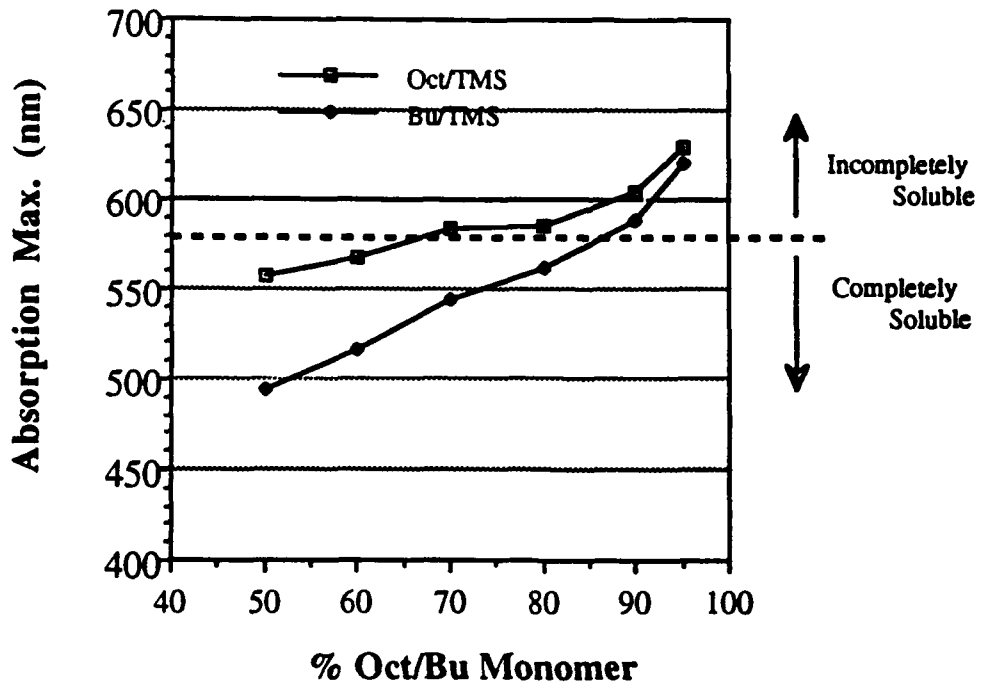

Figure 11

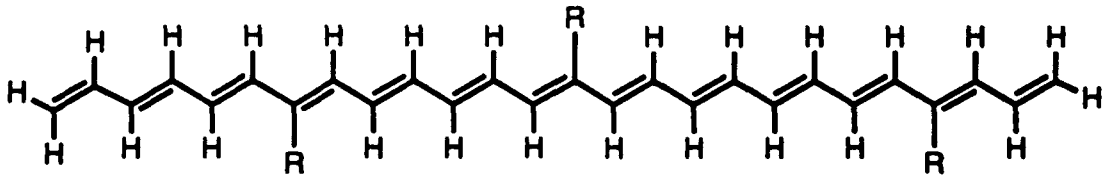

5

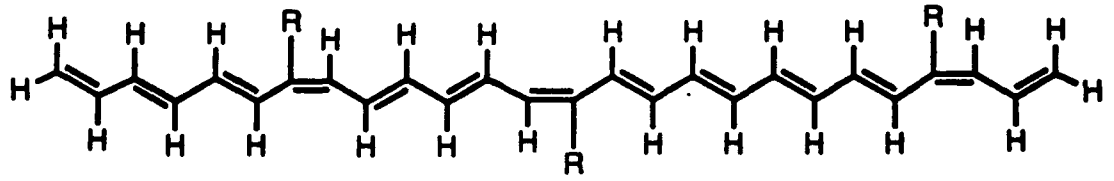

6

Figure 12

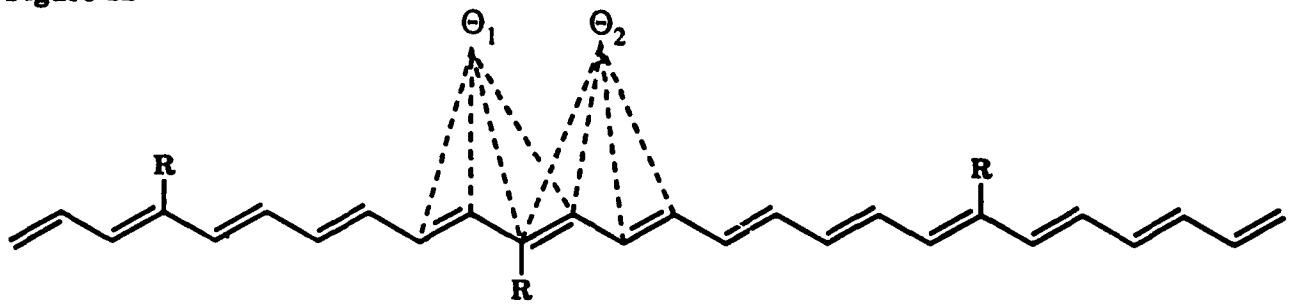

Figure 13

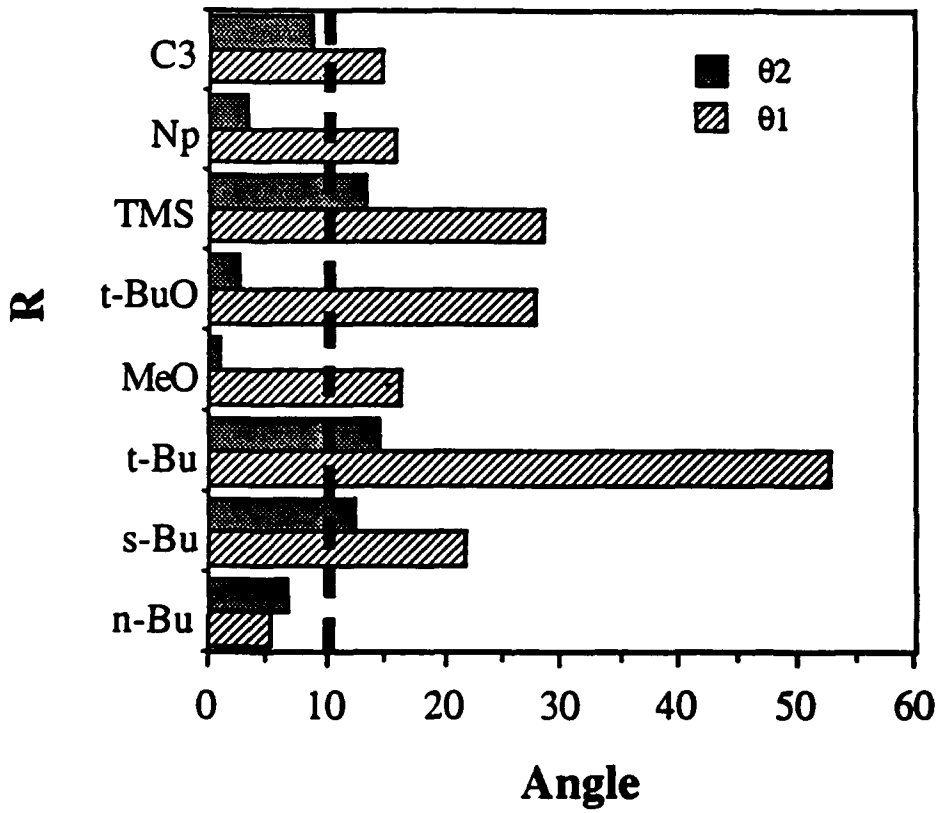

Figure 14

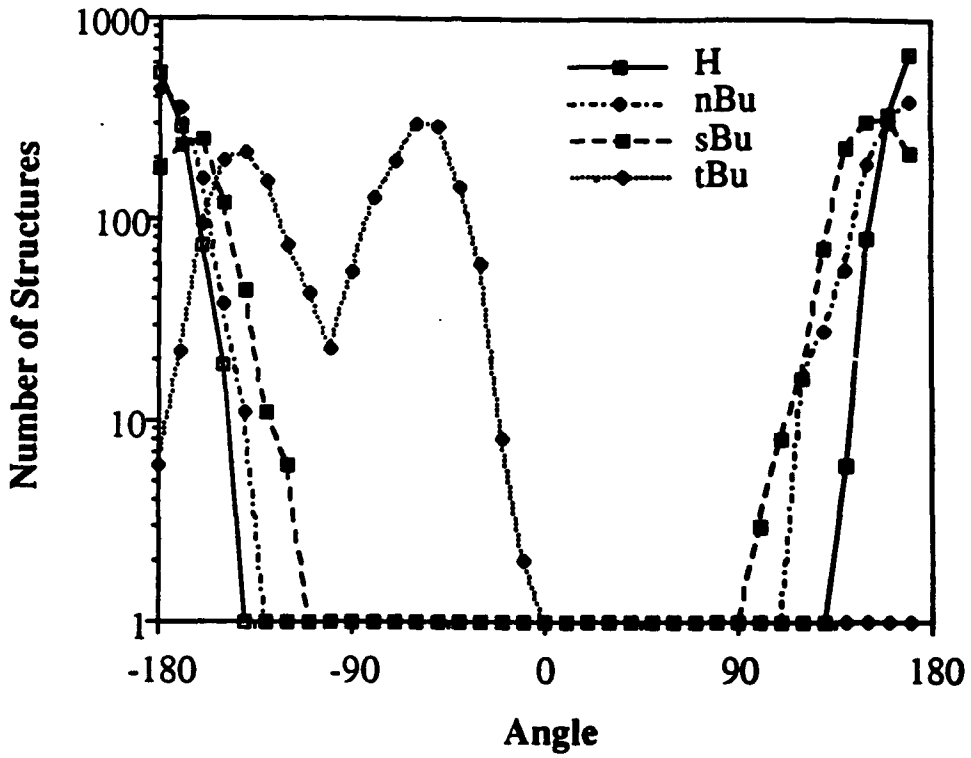

Figure ~~15~~ 16

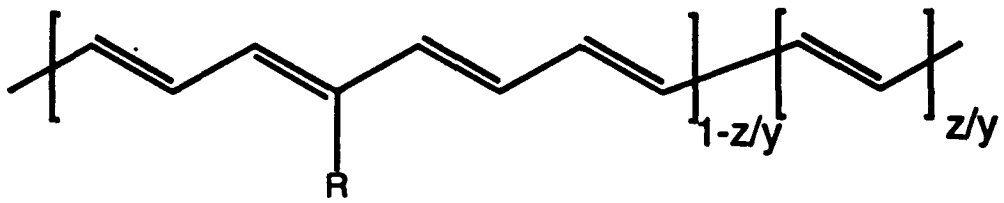

Figure ~~1~~ 15

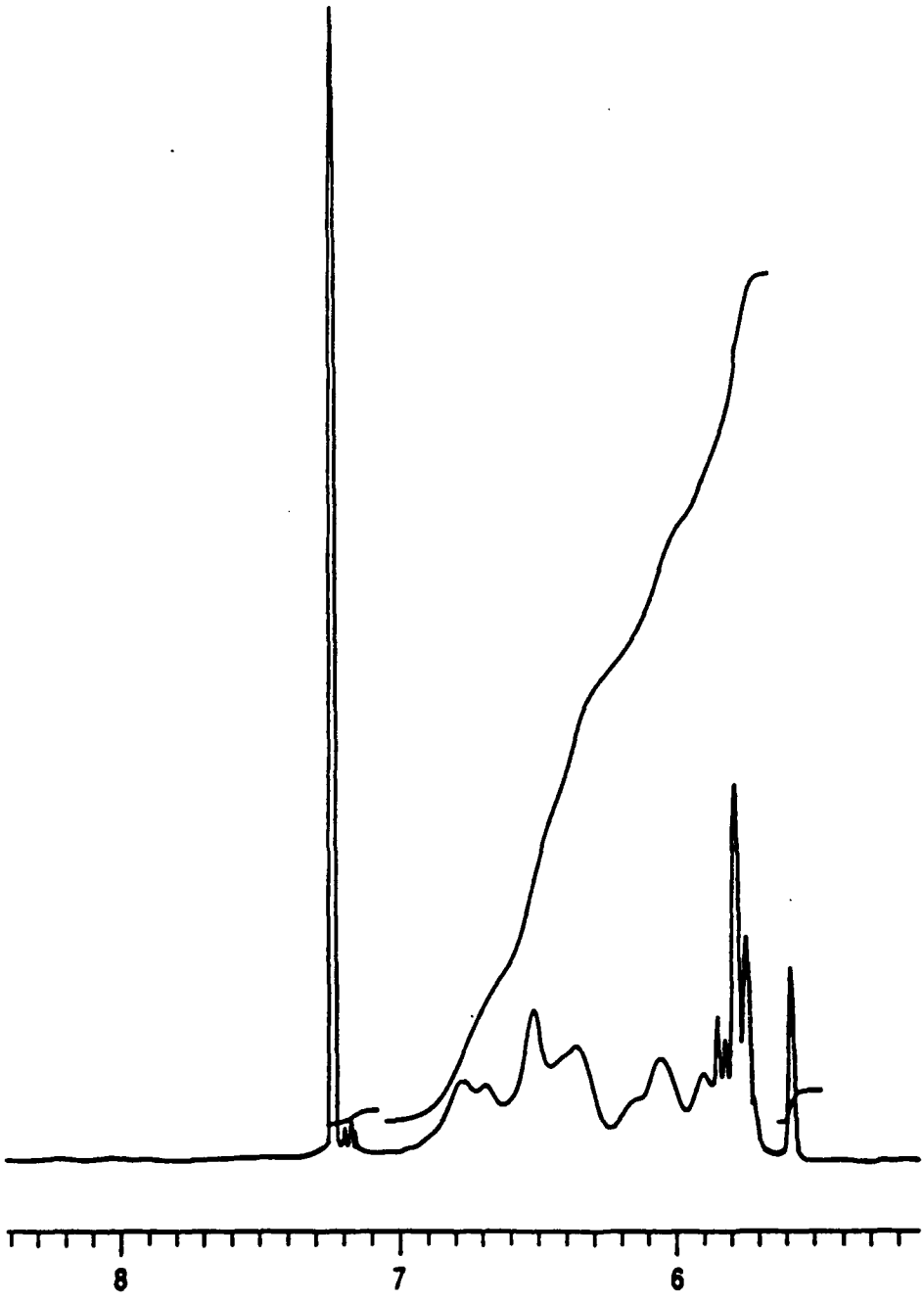

Table 1. Molecular weights (GPC) of the cis polymers[a]

R	M_n(x 10^{-3})	M_w (x 10^{-3})	PDI
n-Butyl	2.9	13.8	4.7
n-Octyl	47	111	2.5
n-Octadecyl	14	46	3.2
Neopentyl	93	132	1.4
2-Ethylhexyl	238	360	1.5
t-Butoxy	252	341	1.4
Phenyl	233	345	1.5
s-Butyl	24.8	49.5	2.0
t-Butyl	25	42	1.7
Isopropyl	10.0	58.0	5.7
Cyclopentyl	16.0	121.7	7.6
Cyclopropyl	20.4	52.4	2.6

[a]Synthesized with catalyst **3** at monomer/catalyst = 150±10:1.

Table 2. Differences in the heat of formation of isomers of **4**.

R	ΔH_f[a] (cc→ct)	ΔH_f[a] (ct → tt)	ΔH_f[a] (cc → tt)
H	-1.20	-1.13	-2.33
n-Butyl	-2.37	+2.00	-0.37
s-Butyl	-1.39	+2.21	+0.83
t-Butyl	-1.64	+2.22	+0.58
MeO	-0.06	-0.30	-0.36
t-BuO	-2.65	+0.57	-2.08
TMS	-0.95	+0.96	+0.01
Np	-1.19	-0.56	-1.76

[a]in kcal/mol

Table 3. Visible absorption, Raman, electrical conductivity and differential scanning calorimetry data.

R	λ_{cis} (nm)[a]	λ_{trans} (nm)[a]	ν_1 A_g(C-C) (cm^{-1})	ν_2 A_g(C=C) (cm^{-1})	σ (Ω^{-1}/cm)	y[b]	T_{isom}[c]
H[d]	—[e]	—[e]	1113	1491	50-350	0.17	150
Methyl	—[e]	—[e]	1126-1132	1516	15-44	—[f]	103
n-Butyl	462	614§	1132	1514	0.25-0.7	0.10-0.13	107
n-Octyl	480	632§	1114-1128	1485	15-50	0.11-0.19	102
n-Octadecyl	538	630§	—[f]	—[f]	0.60-3.65	0.14-0.16	102
Neopentyl	412	634§	1131	1509	0.2-1.5[k]	0.10-0.18[k]	110
					15-21[h]	0.13-0.17[h]	
2-Ethylhexyl	—[b]	616§	1128	1507	—[f]	—[f]	—[f]
Methoxy	—[e]	—[e]	1126-1128	1530	3.6-3.9	—[f]	131
					$\times 10^{-3}$		
t-Butoxy	496[i]	594§	1121	1507	$\approx 10^{-7}$	0.11-0.12	116
Phenyl	522	620§			0.3-0.6	0.19-0.28	114
s-Butyl	360	556	1125-1128	1512	1.0-2.0	0.33[k]	122
					$\times 10^{-4}$[k]		
					0.03[j]	0.31[j]	
Isopropyl	306, 366	556	1129	1527	—[f]	—[f]	122
Cyclopentyl	302, 365	550	1131	1533	—[f]	—[f]	119
Cyclopropyl	—[b]	586§	1125[l]	1515[l]	—[f]	—[f]	115
t-Butyl	302	432	1147	1539-1547	$< 10^{-8}$	≈0.03	164
TMS	380	540	1132	1532	0.2	0.12	150

[a] In THF solution. [b]Based upon the molecular formula $(C[H/R]I_y)_x$. [c]From differential scanning calorimetry of solid samples. [d]From reference 35. [e]The solubility of this polymer is too low for this measurement. [f]Not recorded. [§]There is evidence that this material is not a homogeneous solution. Most of this material cannot be filtered through a 0.5 μm filter. [h]After a blue, trans suspension was recast from solution. [i]A typical (mean) value. [j]Film recast from solution. [k]As synthesized (i.e. unisomerized) film. [l]Only a very weak signal was observed.

Table 4. Computed twist angles for model compounds **5** and **6**.[a]

R	**5** MM2		**5** AM1		**6** MM2		**6** AM1	
	Θ_1	Θ_2	Θ_1	Θ_2	Θ_1	Θ_2	Θ_1	Θ_2
n-Bu	5.03	6.50	6.95	7.10	32.50	11.68	50.80	35.31
s-Bu	21.95	12.41	26.49	15.95	36.66	7.92	42.05	32.46
t-Bu	52.74	14.40	64.66	19.18	64.81	3.52	40.67	23.55
MeO	16.48	0.88	18.86	1.01	28.25	6.81	32.70	23.67
t-BuO	27.77	2.67	31.12	1.01	35.36	6.76	40.16	28.34
TMS	28.35	13.26	37.71	10.31	25.46	10.43	25.65	11.61
Phenyl	7.03[b]	4.04[b]	5.08[c]	2.06[c]	19.14[d]	7.51[d]	20.99[e]	7.59[e]
Neopentyl	15.72	3.10	15.49	0.71	49.43	11.82	36.32	28.33
Cyclopentyl	25.35	12.51	25.96	17.76	32.84	7.85	47.61	28.65
Isopropyl	35.83	10.02	24.27	19.12	63.55	2.43	42.47	22.68
Cyclopropyl	14.74	8.74	28.96	11.95	18.01	8.14	24.86	17.10

[a]Angles (in degrees) reported are the absolute value of the supplement of the corresponding dihedral angle and thus denote the degree (but not direction) of twist. $\Theta_x = 0°$ for a planar chain. For R = phenyl, the phenyl ring is twisted out of the plane of the backbone by [b] 65 ° [c] 64 ° [d] 49 ° [e] 48 °.

Scheme 1

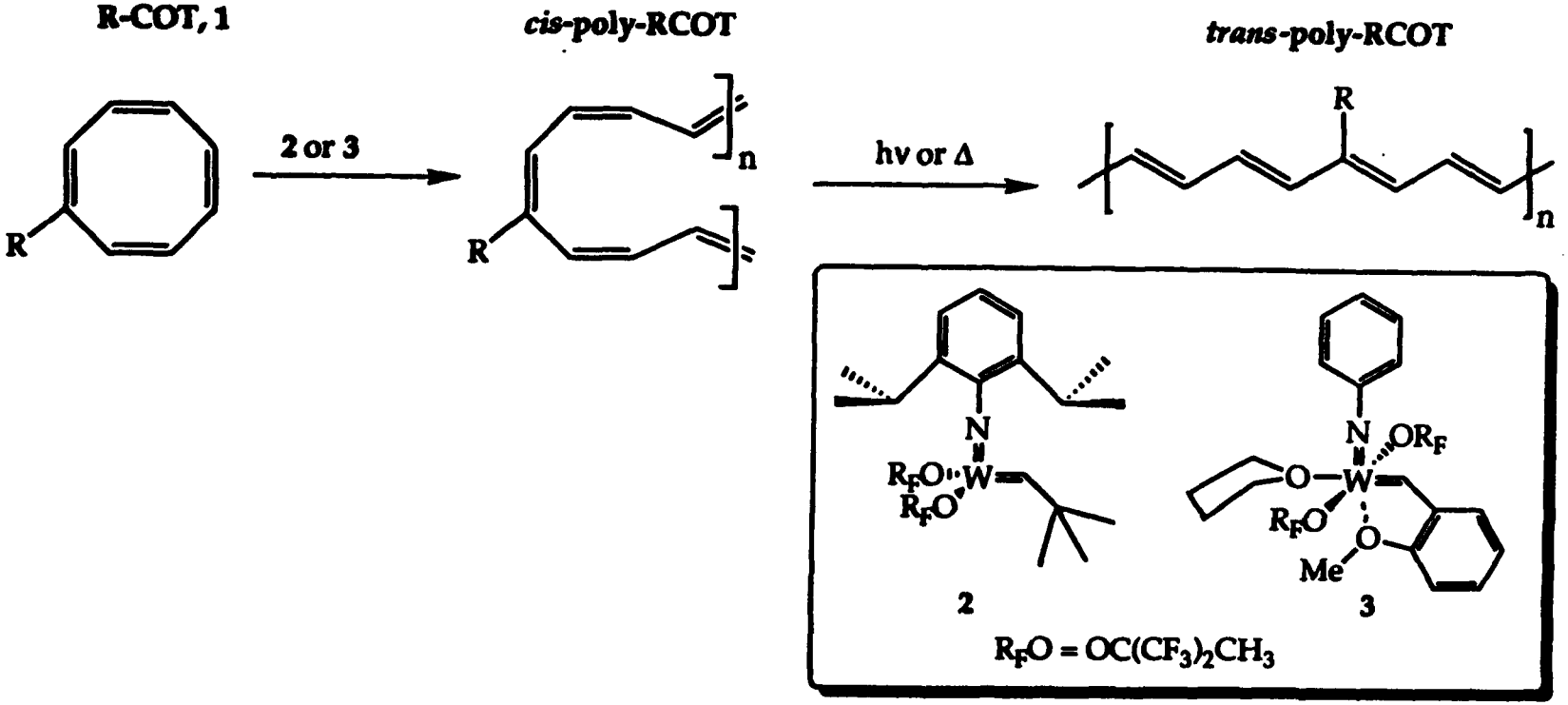
R-COT, 1
cis-poly-RCOT
trans-poly-RCOT
2 or 3
hν or Δ
R
n
N
W
O
Me
2
3
$R_FO = OC(CF_3)_2CH_3$

Scheme 2